Reasoning with Uncertain Points, Straight Lines, and Straight Line Segments in 2D

Jochen Meidow [*,a], Christian Beder [b], Wolfgang Förstner [c]

[a] *FGAN-FOM Research Institute for Optronics and Pattern Recognition, Gutleuthausstr. 1, 76275 Ettlingen, Germany*

[b] *Institute of Computer Science, University of Kiel, Hermann-Rodewald-Str. 3, 24118 Kiel, Germany*

[c] *Institute of Geodesy and Geoinformation, Department of Photogrammetry, University of Bonn, Nußallee 15, 53115 Bonn, Germany*

Abstract

Decisions based on basic geometric entities can only be optimal, if their uncertainty is propagated trough the entire reasoning chain. This concerns the construction of new entities from given ones, the testing of geometric relations between geometric entities, and the parameter estimation of geometric entities based on spatial relations which have been found to hold.

Basic feature extraction procedures often provide measures of uncertainty. These uncertainties should be incorporated into the representation of geometric entities permitting statistical testing, eliminates the necessity of specifying non-interpretable thresholds and enables statistically optimal parameter estimation. Using the calculus of homogeneous coordinates the power of algebraic projective geometry can be exploited in these steps of image analysis.

This review collects, discusses and evaluates the various representations of uncertain

geometric entities in 2D together with their conversions. The representations are extended to achieve a consistent set of representations allowing geometric reasoning. The statistical testing of geometric relations is presented. Furthermore, a generic estimation procedure is provided for multiple uncertain geometric entities based on possibly correlated observed geometric entities and geometric constraints.

Key words: spatial reasoning, uncertainty, homogeneous coordinates, geometric entities

1 Introduction

1.1 Motivation

Geometric entities derived from digital images are inherently uncertain. A rigorous and consistent treatment of these uncertainties is necessary for efficient and successful spatial reasoning in 2D and 3D.

Basic geometric 2D elements are points, straight lines, and straight line segments, especially when observing man-made objects with straight line preserving cameras. These elements are used for calibration, orientation, object localization, object reconstruction, or as parts of intermediate representations for further image interpretation.

This paper is concerned with basic 2D entities. Decisions based on these elements can only be optimal in case the uncertainty is propagated through the reasoning chain. E.g., when using point correspondences for determining the relative orientation of cameras, the parameters of the resulting essential or fundamental matrix

—————
* Corresponding author. Tel.: +49 7243 992 117; fax: +49 7243 992 299
  Email address: `meidow@fom.fgan.de` (Jochen Meidow).

will be uncertain, which needs to be known when reconstructing the objects 3D form. Or, another example, when finding correspondences of points or line segments or when grouping such geometric entities for 3D reconstruction, the quality of all decisions depends on the exploitation of the uncertainty of the given or derived entities.

Reasoning with uncertain geometric entities appears in three forms:

(1) *constructing* new elements from given ones, e.g., when determining the intersection point of two given lines,

(2) *testing* geometric relations between geometric elements, e.g., when checking the collinearity of three points, and

(3) *estimating* parameters of geometric elements based on spatial relations, which have been found to hold, e.g., when fitting a straight line through points which were found to be incident to that line at the same time considering the parallelism to another line.

Obviously, representing geometric entities using homogeneous coordinates, thus exploiting the power of algebraic projective geometry, is of great advantage, especially when using straight line preserving cameras, cf. (Hartley and Zisserman, 2000). This advantage, however, is not so obvious anymore in case the geometric entities are uncertain, cf. (Förstner, 2005): the redundancy of the representation, e.g., three homogeneous coordinates for a point in two dimensions, leads to singular distributions and requires additional constraints during estimation. Moreover, straight line segments are not basic elements of the projective space. They are rather aggregates of geometric entities and no canonical representation seems to exist; e.g., one may choose a point pair or a point together with a direction and a length as representation.

Furthermore, geometric entities with measures of uncertainty which are the result of basic feature extraction procedures are given in representations which require proper transformations into homogeneous entities. Therefore, alternative representations of uncertain geometric entities have to be discussed.

This paper discusses representations of basic uncertain geometric 2D entities together with their use in geometric reasoning. Special emphasis is given to straight lines and straight line segments and their various representations. Especially, straight line segments require an aggregate of entities with different distributions in order to cope with tests on containment and overlap. We restrict our discussion to 2D entities, namely points, straight lines and straight line segments. The generalization to 3D entities is straight forward though involving.

1.2   Previous Work

Exploiting uncertainty for 2D-features has a long history.

Treating the *uncertainty of points* shows the least diversity: Uncertainty is represented by the second moments of the probability density function (p.d.f.), i.e., the covariance matrix Σ_{xx} of the coordinates x. The principle of maximum entropy implies that the coordinates of a point follow a Gaussian distribution. Visualization uses either the confidence ellipse or the ellipse $(x - \mu_x)^\mathsf{T}\Sigma_{xx}^{-1}(x - \mu_x) = 1$ with the bounding box having side lengths $2\sigma_x$ and $2\sigma_y$.

Transferring uncertainty to homogeneous coordinates $\mathbf{x} = [u, v, w]^\mathsf{T}$ has been proposed by several authors, cf. (Collins, 1993; Criminisi, 2001; Kanatani, 1995). The Bingham distribution (Bingham, 1974), useful for bi-directional data, thus unoriented homogeneous vectors, usually is replaced by a Gaussian distribution. How-

4

ever, requiring that homogeneous entities have singular covariance matrices in all cases leads to inconsistencies and does not reflect the true nature of homogeneous vectors, namely being linear subspaces in $\mathbb{R}^2$, thus only representing the direction $\lambda \mathbf{x}$.

Unfortunately only few image processing methods for extracting interest points yield covariances as, e.g., the one in (Förstner and Gülch, 1987). The validity of such covariances has often be discussed. A study into the accuracy of corner points is contained in (Rohr, 1992). The bias of point detectors has been discussed in (Schmid et al., 2000). Suggestions for simplifications, such as assuming independent and identically distributed coordinates are common. A discussion of the effect of such simplifications has been done in (Kanazawa and Kanatani, 2001), however not taking into account the fact that point operators do not necessarily lead to points with round confidence ellipses, e.g., when following the proposal of Köthe (2003) who requires the smallest eigenvalue to show a local maximum.

Uncertain straight lines have received increasing interest. Also here a covariance matrix Σ_{ll} may be used to represent the p.d.f. of the two line parameters. As they usually represent the position and the direction of the line in some way, e.g., using the distance d of the line from the origin and the direction ϕ of the normal in the Hessian form, the dimension of the two standard deviations differ, e.g., being radiants and meters or pixels, respectively. As direct visualization of the covariance matrix $\Sigma(\phi, d)$ is not intuitive, visualization of the line uncertainty is usually done by the confidence hyperbola, representing the confidence regions across the line of all points on the line. The design of the hourglass filter proposed in (Köthe, 2003) follows this characteristic. Early discussions of the uncertainty of a 2D straight line described by such a hyperbolic error band can be found in (Wolf, 1938). This repre-

sentation has repeatedly been used for visualization (Faugeras, 1993) especially of epipolar lines, cf. (Zhang, 1998; Ochoa and Belongie, 2006). Furthermore, Utcke (1998) shows the advantages for the representation of a straight line with its centroid, which leads to a representation analogous to uncertain points.

Straight line segments with attached uncertainty are used frequently, especially for 3D-reconstruction of man made objects, cf. (Noronha and Nevatia, 2001) or for grouping, cf. (Crevier, 1999; Fuchs and Förstner, 1995; Estrada and Jepson, 2004). The uncertainty refers to the position and direction of the straight line as well as to the position of the end points. The uncertainty of the end points is mostly represented using tolerances, often ignoring the uncertainty in direction. In the context of quality measures in geoinformation systems Shi (Shi, 1998; Shi and Liu, 2000) represents uncertainty using standard deviations. The fields used in tensor voting (Guy and Medioni, 1996, 1997) may be interpreted as the p.d.f. of the end points. In contrast to points and straight lines no commonly accepted representation for straight line segments seems to exist. In Section 5 we propose two useful representations for uncertain straight line segments, based on the proposal in (Beder, 2004).

Spatial reasoning with uncertain geometric entities has been explored intensively by Kanatani (1994; 1995). He presents techniques for geometric reasoning using homogeneous representations of geometric entities in 2D and 3D. Singular covariance matrices of joins and intersections in homogeneous coordinates resulting from the normalization of the homogeneous vectors are enforced. Also optimal ML-estimates for lines through collinear uncertain points and intersection points of concurrent uncertain straight lines are given. These estimates are restricted to a single geometric entity and uncorrelated observed geometric entities. The estimation

6

procedure presented in Section 7 covers generalizations to multiple entities and full covariances.

In (Clarke, 1998) solutions for the constrained minimization problems are given using homogeneous coordinates. The shape of the error band of a straight line is discussed as well as the error propagation for the construction of geometric entities and the covariance matrices for homogeneous representations. Compact representations of algebraic projective geometry for representing uncertain geometric entities have been exploited in (Förstner et al., 2000) and used for testing and estimation in (Heuel, 2004). The representation of uncertain axes and directions in $\mathbb{R}^n$ for arbitrary n is intensively discussed in (Mühlich, 2005).

Applying statistical representations of the uncertainty of geometric entities often has been found to make reasoning easier, especially setting thresholds. First attempts are published in (Collins, 1993). By taking into account the uncertainty of image features in the process of grouping, the result of the subsequent object recognition was shown to be enhanced (Utcke, 1998). In (Criminisi, 2001) reasoning with uncertainty is integrated in all steps of image analysis.

1.3   Goals, Outline and Notation

Goals.   The paper has the following goals:

- Collect, discuss and evaluate the various representations for uncertain geometric entities. Such a *review* is missing in the literature but is useful for a large variety of applications.
- Extend the representations to achieve a *consistent set of representations*. This set allows a wide variety of spatial reasoning processes on uncertain geometric

7

entities, especially for constructing new entities and testing spatial relations.

- Provide a generic estimation procedure for *multiple* uncertain geometric entities based on possibly correlated observed geometric entities and geometric constraints. The proposed procedure can handle *uncertain homogeneous vectors* together with possibly singular covariance matrices extending the hitherto known techniques w.r.t. the continuous use of homogeneous representations.

Outline.   The paper is organized as follows: The Sections 2 and 3 discuss the various representations of uncertain 2D points and straight lines. The uncertainties of constructions are derived in Section 4 preparing the representations of uncertain straight line segments given in Section 5. The conversions between these representations are derived. Specific test statistics and hypotheses for various geometric relations between the entities are given in Section 6. The estimation procedure for multiple homogeneous geometric entities is derived and discussed in Section 7.

Notation.   Homogeneous vectors are denoted with upright boldface letters, e.g. $\mathbf{l}$ or $\mathbf{H}$, Euclidean vectors and matrices with slanted boldface letters, e.g. $\boldsymbol{x}$ or $\boldsymbol{R}$. For homogeneous coordinates '=' means an assignment or an equivalence up to a scaling factor $\lambda \neq 0$. We distinguish between the name of a geometric entity denoted by a calligraphic letter, e.g. χ and its representation, e.g., $\boldsymbol{x}$ or $\mathbf{x}$. With the skew-symmetric matrix $\boldsymbol{S}(\boldsymbol{x}) = \boldsymbol{S}_x$ the cross product $\boldsymbol{S}_x \boldsymbol{y} = \boldsymbol{x} \times \boldsymbol{y}$ of two vectors $\boldsymbol{x}$ and $\boldsymbol{y}$ is represented. We make use of the basic rule for variance-covariance propagation: Given the first and second moments $\boldsymbol{\mu}_x$ and Σ_{xx} of a stochastic variable $\underline{\boldsymbol{x}}$ (underscored) the first and second moment of a differentiable function $\underline{\boldsymbol{y}} = \boldsymbol{f}(\underline{\boldsymbol{x}})$ with Jacobian $\boldsymbol{J} = \partial \boldsymbol{f}/\partial \boldsymbol{x}|_{\mu_x}$ are obtained as $\boldsymbol{\mu}_y = \boldsymbol{f}(\boldsymbol{\mu}_x)$ and $\Sigma_{yy} = \boldsymbol{J}\Sigma_{xx}\boldsymbol{J}^\mathsf{T} + O\left(|\Sigma_{xx}|/|\boldsymbol{x}|^2\right)$. This is rigorous for linear functions $\underline{\boldsymbol{y}} = \boldsymbol{J}\underline{\boldsymbol{x}} + \boldsymbol{a}$

8

and a good approximation up to terms of second and higher order if the function is smooth and the variances are small — for a discussion of these approximations cf. (Förstner, 2005). We will use the two-argument version of the arctangent function $\mathrm{atan2}(\cdot, \cdot)$ in case we want to enforce the result to be in the correct quadrant.

2 Representation of Uncertain Points

This section collects Euclidean and homogeneous representations for uncertain 2D points χ most commonly used and their corresponding conversions.

2.1 Euclidean Representations

Among the Euclidean representations we discuss the well-known classical Euclidean representation, namely coordinate pairs, and a centroid form which reflects the uncertain result of feature extraction procedure.

2.1.1 Uncertain Euclidean point

An uncertain Euclidean point in the plane can be represented by the coordinate pair $\boldsymbol{x} = [x, y]^\mathsf{T}$ and its uncertainty by the corresponding covariance matrix

$$
\boldsymbol{\Sigma}_{xx} = \begin{bmatrix} \sigma_x^2 & \sigma_{xy} \\ \sigma_{yx} & \sigma_y^2 \end{bmatrix}.
$$

Thus we have the representation

$$
\boxed{\chi : \quad \{\boldsymbol{x}, \boldsymbol{\Sigma}_{xx}\}} . \tag{1}
$$

9

Observe, that we treat the coordinates $\boldsymbol{x}$ as a sample taken from some arbitrary distribution M characterized by its mean and covariance, thus $\underline{\boldsymbol{x}} \sim M(\boldsymbol{\mu}_x, \boldsymbol{\Sigma}_{xx})$. Of course, $\boldsymbol{x}$ may be also the result of an estimation process together with the corresponding covariance matrix. As a special case, taking a sample results in an estimate for the expected value $\widehat{\boldsymbol{\mu}}_x = \boldsymbol{x}$.

Fig. 1 shows a point and its uncertainty drawn as the *standard* confidence ellipse, being $(\boldsymbol{y} - \boldsymbol{x})^\mathsf{T} \boldsymbol{\Sigma}_{xx}^{-1} (\boldsymbol{y} - \boldsymbol{x}) = 1$ with points $\boldsymbol{y}$ on the ellipse, thus choosing the significance level of the confidence ellipse such that the right side is 1, cf. (Mikhail, 1976, p. 29). [1] The lengths of the semi-axes are the standard deviations $\sigma_u = \sqrt{\lambda_1}$ and $\sigma_v = \sqrt{\lambda_2}$ of the point in a local uv-coordinate system, λ_i being the two eigenvalues of $\boldsymbol{\Sigma}_{xx}$. The angle $\alpha = 1/2 \arctan(2\sigma_{xy}/(\sigma_x^2 - \sigma_y^2))$ denotes the direction of the major axis.

2.1.2 Centroid form

The centroid form is a simple and minimal description of the uncertain point χ and consists of the 5-tuple

$$\boxed{\chi : \quad \{x, y, \alpha;\ \sigma_u, \sigma_v\}}.$$

This representations contains three geometric parameters namely x, y and α, and two standard deviations as parameters in contrast to the above Euclidean representation with two geometric parameters and three statistical parameters to specify the second moments.

Euclidean and centroid representation only differ in their representation of the uncertainty. With the eigenvalues λ_i of $\boldsymbol{\Sigma}_{xx}$ we have $\sigma_u = \sqrt{\lambda_1}$, $\sigma_v = \sqrt{\lambda_2}$, and

---

[1] A representation for the error ellipse in homogeneous coordinates is given below.
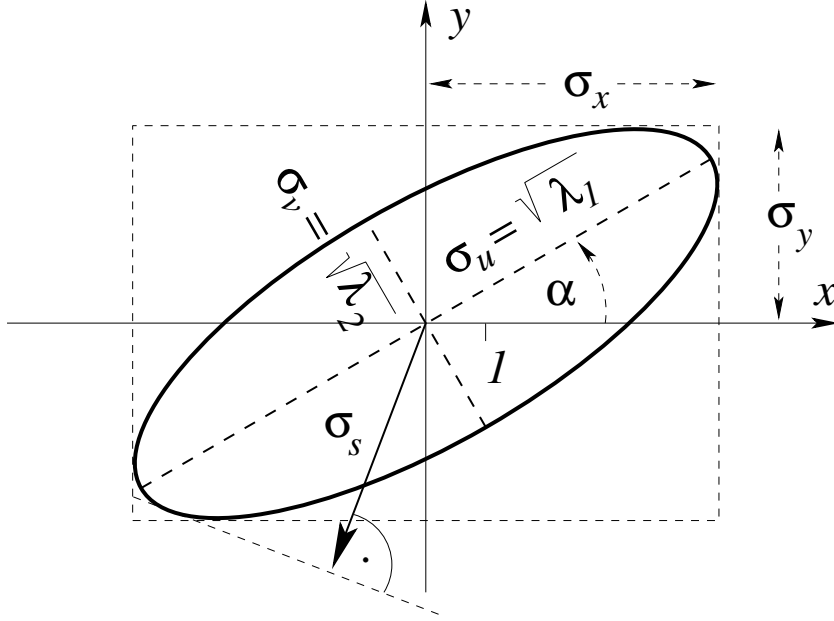
Fig. 1. A point and its standard confidence ellipse. The semi-axes are the minimum and maximum directional standard deviations. The standard deviation σ_s into an arbitrary direction is given by the distance from the origin to the tangent of the ellipse perpendicular to that direction. Therefore, the bounding box has side lengths $2\,\sigma_x$ and $2\,\sigma_y$, adapted from (Mikhail, 1976, p. 29).

$\alpha = 1/2 \arctan(2\sigma_{xy}/(\sigma_x^2 - \sigma_y^2))$. For the inverse transformation we simply need to rotate the axis-parallel ellipse with covariance matrix $\mathrm{Diag}\,(\sigma_u^2, \sigma_v^2)$ by α.

2.2 *Homogeneous Representations*

Using homogeneous coordinates for representing geometric entities is of great advantage for spatial reasoning. The pure homogeneous representation of a point as a vector, possibly normalized, is presented. Furthermore, we discuss the conic form which represents the standard confidence region as a homogeneous matrix. This implicit representation may be used e.g. as interface for a plotting routine accepting general conics.

2.2.1 *Homogeneous Vector and its Covariance Matrix*

The homogeneous representation of a point χ is

$$\boxed{\chi : \quad \{\mathrm{x}, \boldsymbol{\Sigma}_{\mathrm{xx}}\}} \,. \tag{2}$$

The homogeneous coordinates of points in the plane are the elements of the 3-vectors

$$\mathbf{x} = \left[\begin{array}{c} \boldsymbol{x}_0 \\ \hline x_h \end{array}\right] = \left[\begin{array}{c} u \\ \hline v \\ \hline w \end{array}\right] := \left[\begin{array}{c} \lambda x \\ \hline \lambda y \\ \hline \lambda \end{array}\right] \tag{3}$$

subject to the constraint $|\mathbf{x}|^2 = u^2 + v^2 + w^2 \neq 0$. When deriving homogeneous coordinates from Euclidean coordinates, the factor $\lambda \neq 0$ can be chosen arbitrarily, either as fixed or stochastic value. Homogeneous coordinates with $w = 0$ represent points at infinity. The vector $\mathbf{x}$ can be split into an Euclidean part $\boldsymbol{x}_0$ and a homogeneous part x_h.

The covariance matrix $\boldsymbol{\Sigma}_{\mathrm{xx}}$ of the homogeneous coordinates $\underline{u}$, $\underline{v}$ and $\underline{w}$ has in general rank 3, unless certain constraints are imposed on $\underline{\mathbf{x}}$. We will see below, that plain variance propagation may lead to both, full rank and singular matrices for homogeneous coordinates, cf. the dicussion in (McGlone et al., 2004) and (Förstner, 2005).

12

For the transformation equations $\mathbf{x} \rightarrow \boldsymbol{x} : x = u/w$ and $y = v/w$ the corresponding Jacobian at $\mathbf{x}$ reads

$$J(\mathbf{x}) = \frac{\partial \boldsymbol{x}}{\partial \mathbf{x}} = \begin{bmatrix} \dfrac{1}{w} & 0 & -\dfrac{u}{w^2} \\ 0 & \dfrac{1}{w} & -\dfrac{v}{w^2} \end{bmatrix}$$

leading to the covariance matrix $\Sigma_{xx} = J(\boldsymbol{\mu}_{\mathrm{x}})\Sigma_{\mathrm{xx}}J^{\top}(\boldsymbol{\mu}_{\mathrm{x}})$.

For the inverse transformation $[\boldsymbol{x}, \lambda] \rightarrow \mathbf{x}$, which includes the possibly stochastic factor λ, we have the Jacobian

$$J_{h,e\lambda} = \frac{\partial \mathbf{x}}{\partial \boldsymbol{x}}, \frac{\partial \mathbf{x}}{\partial \lambda} = \begin{bmatrix} \lambda & 0 & x \\ 0 & \lambda & y \\ 0 & 0 & 1 \end{bmatrix}$$

because of the Eq. 3. This leads to the covariance matrix

$$\Sigma_{\mathrm{xx}} = J_{h,e\lambda}(\boldsymbol{x}, \lambda) \begin{bmatrix} \Sigma_{xx} & \Sigma_{x\lambda} \\ \Sigma_{\lambda x} & \sigma_{\lambda}^2 \end{bmatrix} J_{h,e\lambda}^{\top}(\boldsymbol{x}, \lambda)$$

assuming λ to be stochastic and possibly correlated to $\boldsymbol{x}$.

In case Σ_{xx} is regular, Σ_{xx} has rank three only if the factor $\underline{\lambda}$ is assumed to be stochastic and if it is not 100 % correlated with the coordinates.

Only when assuming λ to be deterministic, we obtain the classical singular covariance matrix of a homogeneous point (Criminisi, 2001)

$$\Sigma_{\mathrm{xx}} = \lambda^2 \begin{bmatrix} \sigma_x^2 & \sigma_{xy} & 0 \\ \sigma_{yx} & \sigma_y^2 & 0 \\ 0 & 0 & 0 \end{bmatrix} = \lambda^2 \begin{bmatrix} \Sigma_{xx} & \mathbf{0} \\ \mathbf{0}^{\mathsf{T}} & 0 \end{bmatrix}. \tag{4}$$

2.2.2 Conic representation of a point

A further representation of an uncertain point is the confidence ellipse represented as homogeneous symmetric matrix

$$\boxed{\mathcal{X}: \quad \mathbf{C}_{\mathrm{xx}}}$$

as plotted in Fig. 1. This representation uses the fact that each conic can be represented by a 3×3-matrix when using homogeneous coordinates and results in an implicit representation for both the mean and the covariance matrix. Thus for points with homogeneous coordinates $\mathbf{y} = [u, v, w]^{\mathsf{T}}$, which sit on a conic we have $au^2 + bv^2 + 2cuv + 2duw + 2evw + fw^2 = 0$ or $\mathbf{y}^{\mathsf{T}}\mathbf{C}_{\mathrm{xx}}\mathbf{y} = 0$ with the matrix

$$\mathbf{C}_{\mathrm{xx}} = \begin{bmatrix} a & c & d \\ c & b & e \\ d & e & f \end{bmatrix}.$$

The uncertainty of the homogeneous 3-vector $\mathbf{x}$ can be represented by the 3×3-covariance matrix Σ_{xx} in the (u, v, w)-space. The covariance matrix again can

14

be represented as an ellipsoid $\mathcal{E}$ being a special type of a quadric $\mathcal{Q}$, cf. Fig. 2. If centered at $\mathbf{0}$, $\mathcal{E}$ is represented as $\mathbf{y}^\mathsf{T}\boldsymbol{\Sigma}_{\mathrm{xx}}^{-1}\mathbf{y} = k^2$ with $\mathbf{y} = [u, v, w]^\mathsf{T}$ and k depending on the significance level. When viewed from the origin, the contour of the ellipsoid in the (x, y)-plane $w = 1$ is a conic.
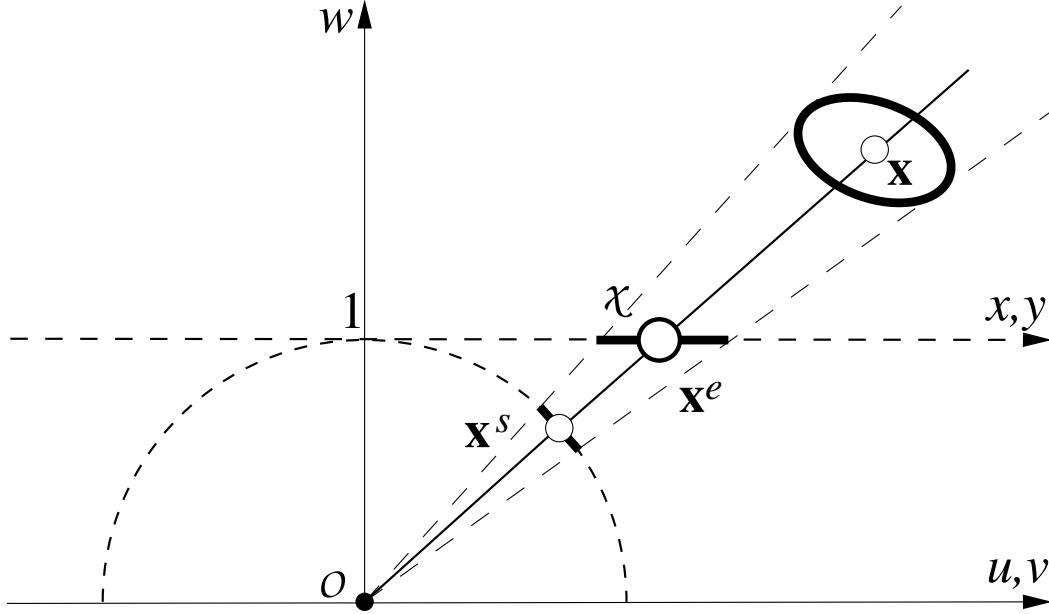

Fig. 2. Euclidean and spherical normalization. The Euclidean (x, y)-plane is embedded in the 3D (u, v, w)-space, sitting at $w = 1$. Normalization is projection to the plane $w = 1$ or to the unit sphere respectively. The uncertainty of the the 3-vector $\mathbf{x}$ is represented as an ellipsoid. Its projection leads to singular 3×3-covariance matrices, indicated by the flat line segments. The equivalence of the representations is guaranteed in case the uncertainty of the direction from the origin O is the same.

For the conversion from the purely homogeneous representation to the conic representation we consider the quadric representation of the ellipsoid $\mathcal{E}$ which can be either use the points $\mathcal{Y}$ with their homogeneous coordinates $\mathbf{Y}$ on the ellipsoid or the tangent planes $\mathcal{A}$ to the ellipsoid with their homogeneous coordinates $\mathbf{A}$, i.e.

$$\mathcal{Q}: \quad \mathbf{Y}^\mathsf{T}\mathbf{Q}\mathbf{Y} = 0 \quad \text{or} \quad \mathbf{A}^\mathsf{T}\mathbf{Q}^*\mathbf{A} = 0 \tag{5}$$

15

where $\mathbf{Q}^*$ is the adjoint matrix of the 4×4-quadric matrix $\mathbf{Q}$. The second representation is to be preferred here, as we do not want to restrict to regular quadrics.

With $\mathbf{Y} = \lambda[\mathbf{y}^\mathsf{T}, 1]^\mathsf{T}$ and $\mathbf{Q}(k) = \mathrm{Diag}\left(k^{-2}\boldsymbol{\Sigma}_{\mathrm{xx}}^{-1}, -1\right)$ the equivalence is given and the dual quadric is the symmetric 4×4-matrix

$$
\mathbf{Q}^*(k) = \begin{bmatrix} k^2\boldsymbol{\Sigma}_{\mathrm{xx}} & \mathbf{0} \\ \\ \mathbf{0}^\mathsf{T} & -1 \end{bmatrix} \tag{6}
$$

which describes the confidence region also in case $\boldsymbol{\Sigma}_{\mathrm{xx}}$ is singular. Eq. 6 represents the confidence ellipsoid of the stochastic homogeneous vector $\underline{\mathbf{x}}$ however centred at the origin.

We now want to determine the confidence ellipse of $\underline{x}$ in the plane $w = 1$. It represents the uncertainty of the Euclidean coordinates $[x, y]^\mathsf{T}$. Equivalently we may represent the uncertainty by the direction of the line through the origin and the point $[x, y, 1]^\mathsf{T}$, which may be visualized by a confidence cone centred at the origin and being tangential to the confidence ellipsoid of the point $\underline{\mathbf{x}} = [\underline{u}, \underline{v}, \underline{w}]^\mathsf{T}$. Therefore the confidence ellipse may be derived treating the origin as the projection centre of a pinhole camera with the plane $w = 1$ as image plane and projecting the ellipsoid into the apparent contour in the image plane $w = 1$.

This geometric configuration of the origin, the image plane $w = 1$, and the confidence ellipsoid can be shifted such that the confidence ellipsoid sits in the origin and the centre of the projection is at $-\mathbf{x}$. Then the central projection of a point $[u, v, w]$ onto the plane $w = 1$ can be represented by the 3×4 projection matrix $\mathbf{P} = [\boldsymbol{I}_3| - \mathbf{x}]$. Without proof (cf. Hartley and Zisserman, 2000, p. 201) the contour $\mathcal{C}$ of a general quadric $\mathcal{Q}$ can be determined by $\mathbf{C} = (\mathbf{P}\mathbf{Q}^*\mathbf{P}^\mathsf{T})^*$. Thus the conic is

$\mathbf{C}_{\mathrm{xx}}(k) = \left(k^2 \Sigma_{\mathrm{xx}} - \mathbf{xx}^\mathsf{T}\right)^*$ and with $k = 1$ we obtain the standard conic centred at $\mathbf{x}$

$$\mathbf{C}_{\mathrm{xx}} = \left(\Sigma_{\mathrm{xx}} - \mathbf{xx}^\mathsf{T}\right)^*. \tag{7}$$

This relation is valid for a general covariance matrix Σ_{xx} and thus generalizes the literally identical relation given in (Ochoa and Belongie, 2006), where the derivation uses the standard form of the covariance matrix in Eq. 4.

For the conversion of the conic to the centroid representation the homogeneous matrix $\mathbf{C}_{\mathrm{xx}} = (C_{ij})$ of a conic representing a standard confidence ellipse can be decomposed, leading to the angle

$$\phi = \frac{1}{2} \arctan\left(2C_{12}/(C_{22} - C_{11})\right) \tag{8}$$

and the centroid

$$\boldsymbol{x}_0 = - \begin{bmatrix} C_{11} & C_{12} \\ C_{21} & C_{22} \end{bmatrix}^{-1} \begin{bmatrix} C_{13} \\ C_{23} \end{bmatrix} = -\boldsymbol{C}^{-1}\boldsymbol{c}. \tag{9}$$

The standard deviations σ_u and σ_v relate to the eigenvalues λ_i of the centered conic $\mathbf{C}/C_{33}$ where $\mathbf{C} = (C_{ij}) = \mathbf{M}^{-\mathsf{T}} \mathbf{C}_{\mathrm{xx}} \mathbf{M}^{-1}$ with the motion matrix

$$\mathbf{M} = \begin{bmatrix} \boldsymbol{R}_\phi & \boldsymbol{x}_0 \\ \mathbf{0}^\mathsf{T} & 1 \end{bmatrix}. \tag{10}$$

We obtain $\sigma_u = \sqrt{\lambda_1}$ and $\sigma_v = \sqrt{\lambda_2}$.

2.2.3 Normalization

The ambiguity of the homogeneous representation may be eliminated by normalization. One usually distinguishes Euclidean and spherical normalization. The resultant uncertain 3-vectors are still homogeneous, however, due to the normalization they are guaranteed to have a rank 2 covariance matrix. Normalizations lead to further homogeneous representations. They can be used as a surrogate of Eq. 2. We therefore directly give the corresponding Jacobians and covariances here.

Euclidean Normalization. Homogeneous coordinates of a point can be transformed into Euclidean coordinates with the relation in Eq. 3. The corresponding Euclidean normalization operation

$$\mathbf{x}^e = \mathsf{N}_e(\mathbf{x}) = \mathbf{x}/x_h \tag{11}$$

transforms the homogeneous vector such that its homogeneous part has the Euclidean norm 1. To extend the normalization operation to uncertain points, variance propagation has to be applied to Eq. 11. With the Jacobian evaluated at $\mathbf{x}$

$$\boldsymbol{J}_e(\mathbf{x}) = \frac{\partial \mathsf{N}_e(\mathbf{x})}{\partial \mathbf{x}} = \frac{1}{x_h^2} \begin{bmatrix} x_h \boldsymbol{I}_2 & -\boldsymbol{x}_0 \\ \\ \mathbf{0}^\mathsf{T} & 0 \end{bmatrix}$$

this normalization in our special case reads

$$\chi : \quad \{\mathbf{x}^e, \Sigma_{\mathrm{xx}}^e\} = \left\{ \mathbf{x}/x_h, \quad \boldsymbol{J}_e(\boldsymbol{\mu}_{\mathrm{x}})\Sigma_{\mathrm{xx}}\boldsymbol{J}_e^\mathsf{T}(\boldsymbol{\mu}_{\mathrm{x}}) \right\}.$$

as the variance propagation requires the Jacobians to be taken at the expected values.

Spherical Normalization. Normalization of a homogeneous vector **x** to unit length with the help of the operator

$$\mathsf{N}_s(\mathbf{x}) = \mathbf{x}/|\mathbf{x}| \tag{12}$$

is called spherical normalization, whereas $|\cdot|$ denotes the vector norm. This normalization operation is identical for all geometric entities and will be presented here exemplary for a point **x**. For the result all coordinates are lying on the unit sphere S^2 being a classical representation of the projective plane $\mathbb{P}^2$. The orientation of the vector is preserved.

Employing variance propagation with the Jacobian at **x**

$$\boldsymbol{J}_s(\mathbf{x}) = \frac{\partial \mathsf{N}_s(\mathbf{x})}{\partial \mathbf{x}} = \frac{1}{|\mathbf{x}|} \left[\boldsymbol{I}_3 - \frac{\mathbf{x}\mathbf{x}^\mathsf{T}}{\mathbf{x}^\mathsf{T}\mathbf{x}} \right]$$

this normalization operation reads

$$\chi: \quad \{\mathbf{x}^s, \Sigma_{\mathrm{xx}}^s\} = \left\{ \mathbf{x}/|\mathbf{x}|, \quad \boldsymbol{J}_s(\boldsymbol{\mu}_{\mathrm{x}}) \Sigma_{\mathrm{xx}} \boldsymbol{J}_s^\mathsf{T}(\boldsymbol{\mu}_{\mathrm{x}}) \right\}.$$

The ambiguity with respect to the sign of the normalization has no effect on the result of the error propagation.

2.2.4 Conditioning

In order to avoid numerical difficulties, homogeneous entities should be transformed such that the Euclidean part is significantly smaller than the homogeneous part, cf. (Hartley, 1997). This transformation is called *conditioning* as the condition number of the resulting matrix is closer to 1. One way is to apply a translation and

19

a scaling leading to the representation

$$\chi: \quad \{\mathbf{x}^c, \Sigma^c_{\mathrm{xx}}\} = \{\mathbf{T}_c\mathbf{x}, \quad \mathbf{T}_c\Sigma_{\mathrm{xx}}\mathbf{T}_c^\mathsf{T}\}$$

with the homography

$$\mathbf{T}_c = \begin{bmatrix} 1 & 0 & -x_c \\ 0 & 1 & -y_c \\ 0 & 0 & s \end{bmatrix} \tag{13}$$

containing adequate parameters, e.g., the centroid $[x_c, y_c]^\mathsf{T}$ of all points of concern and the maximum distance s of these points to this centroid. Conditioning is also of major importance when estimating geometric entities, cf. Section 7.

3   Representation of Uncertain Straight Lines

3.1   Euclidean Representations

Of the various Euclidean representations of a 2D straight line l (Bronstein and Semendjajew, 1991) we only discuss two, the Hessian normal form and a special point-direction form.

3.1.1 *Hessian normal form.*

With the direction ϕ of the normal to the straight line and the distance d of the line to the origin the *Hessian normal form*

$$x \cos(\phi) + y \sin(\phi) - d = 0 \tag{14}$$

can be specified. We obtain the representation

$$\boxed{\ell: \quad \{\boldsymbol{h}, \boldsymbol{\Sigma}_{hh}\}}$$

with the parameters $\boldsymbol{h} = [\phi, d]^{\mathsf{T}}$ and the covariance matrix

$$\boldsymbol{\Sigma}_{hh} = \begin{bmatrix} \sigma_\phi^2 & \sigma_{\phi d} \\ \\ \sigma_{d\phi} & \sigma_d^2 \end{bmatrix},$$

where in general $\sigma_{\phi d} \neq 0$ holds. The visualization of the parameter vector $[\phi, d]$ as point leads to the well-known Hough representation (Duda and Hart, 1972). With the Hessian normal form an uncertain straight line ℓ therefore can be represented by the 5-tuple

$$\ell: \quad \{\phi, d;\ \sigma_\phi, \sigma_d, \sigma_{\phi d}\}.$$

The uncertain straight line can be visualized by the set of all 1D-confidence regions of points on the line measured across the line. This establishes the confidence region of the uncertain line. It has a hyperbolic shape. It can be shown to be identical to the envelope of all lines represented by the points on the standard confidence ellipse of $\boldsymbol{\Sigma}_{hh}$.

The confidence region can be determined from the standard deviation σ_n of the distance $\underline{n} = x\cos(\underline{\phi}) + y\sin(\underline{\phi}) - \underline{d}$ of some fixed point $[x, y]^{\mathsf{T}}$ from the line. It is given by $\sigma_n^2(m) = m^2\sigma_\phi^2 + 2m\sigma_{\phi d} + \sigma_d^2$ with the distance $m = x\sin(\phi) - y\cos(\phi)$ of the point along the line, measured from the point χ_f on the line closest to the origin (cf. Fig. 3). The minimum standard deviation $\sigma_q = \min_m(\sigma_n(m))$ is reached at the point χ_0 with

$$m_0 = -\frac{\sigma_{\phi d}}{\sigma_\phi^2}, \quad \sigma_\phi > 0 \tag{15}$$

and has the value $\sigma_q^2 = \sigma_d^2 - \sigma_{\phi d}^2/\sigma_\phi^2$. In case we use the confidence regions $(-\sigma_n, +\sigma_n)$ we obtain the standard confidence region for the uncertain line.

3.1.2 Centroid Representation

The above suggests a centroid representation for lines analogue to the centroid representation for points. Its centroid is the point χ_0 with the representation $[x_0, y_0]^{\mathsf{T}}$. In addition we use the direction $\alpha = \phi - \pi/2$ of the line. This fixes a local mn-coordinate system where the m-axis points in the direction of the line and n in the direction of its normal, pointing to the left side of the line. The standard deviation σ_α of the direction and the minimum standard deviation σ_q across the line define the standard confidence region.

The centroid representation of a straight line thus consists of the 5-tuple

$$\boxed{l: \quad \{x_0, y_0, \alpha;\ \sigma_\alpha, \sigma_q\}} . \tag{16}$$

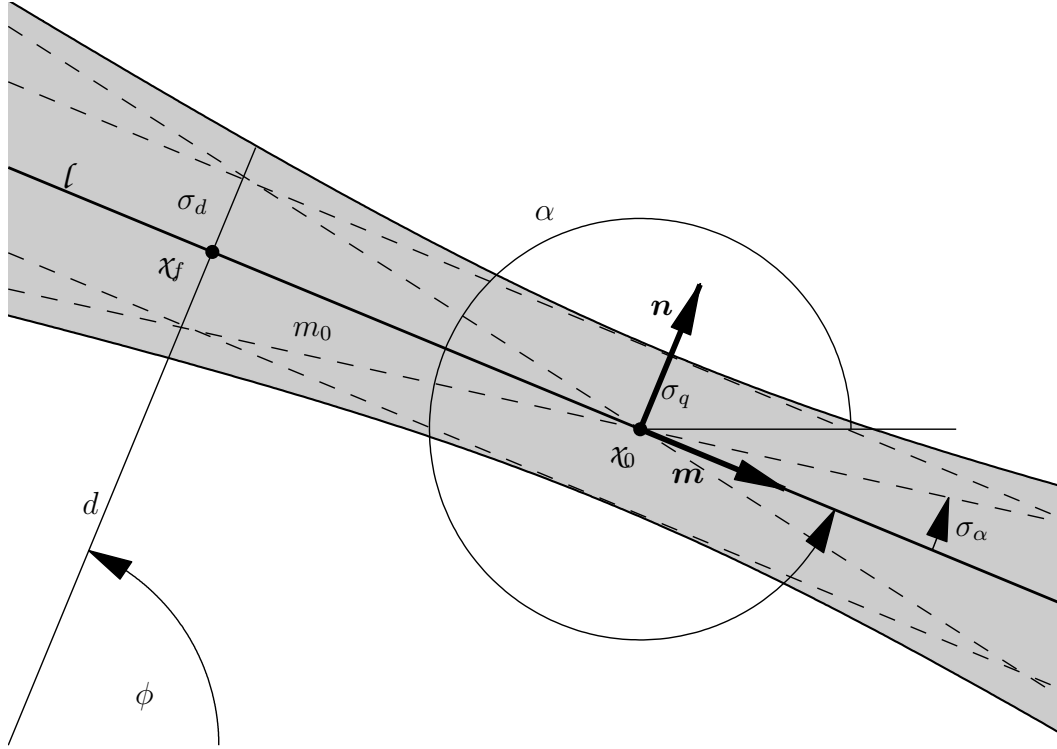The parameters of the centroid form (Eq. 16) with $\alpha = \phi - \pi/2$ result from the

22

Fig. 3. Uncertain straight line l and its hyperbolic error band. The point χ_f has the shortest distance d to the origin and a distance of m_0 to the point χ_0 with smallest standard deviation σ_q across the line with the orientation $\phi = \alpha + \pi/2$. The position of the point with the lowest variance σ_q^2 depends on the covariance $\sigma_{\phi d}$. For $\sigma_q = 0$ and $\sigma_\alpha = 0$ resp. the dashed lines form the error region.

Hessian normal form via the transformation

$$
\begin{bmatrix} x_0 \\ y_0 \end{bmatrix} = \boldsymbol{R}_\alpha^\mathsf{T} \begin{bmatrix} m_0 \\ d \end{bmatrix}
$$

with the location $[m_0, d]$ (cf. Eq. 15) of the centroid in a coordinate system situated in the origin and being parallel to the mn-system.

23

The parameters of the Hessian normal form result from the centroid form with

$$
\begin{bmatrix} m_0 \\ d \end{bmatrix} = \boldsymbol{R}_\alpha \begin{bmatrix} x_0 \\ y_0 \end{bmatrix},
$$

$\phi = \alpha + \pi/2$, $\sigma_{\phi d} = -m_0 \sigma_\phi^2$ (cf. Eq. 15), and $\sigma_d^2 = m_0^2 \sigma_\phi^2 + \sigma_q^2$.

3.2 Homogeneous Representations

3.2.1 Homogeneous Vector and its Covariance Matrix

The homogeneous representation of the uncertain line is given by

$$
\ell : \quad \{\mathbf{l}, \Sigma_{\mathrm{ll}}\}
$$

with the 3-vector

$$
\mathbf{l} = \begin{bmatrix} \boldsymbol{l}_h \\ \overline{} \\ l_0 \end{bmatrix} = \begin{bmatrix} a \\ b \\ \overline{} \\ c \end{bmatrix} := \lambda \begin{bmatrix} \cos(\phi) \\ \sin(\phi) \\ \overline{} \\ -d \end{bmatrix} \tag{17}
$$

subject to the constraint $a^2 + b^2 + c^2 \neq 0$. In case the homogeneous coordinates are derived from the Hessian normal form the factor $\lambda \neq 0$ can be chosen arbitrarily, either fix or stochastic. In case $a^2 + b^2 = 0$ we obtain the line at infinity. The Euclidean part l_0 obviously depends on the origin of the coordinate system, whereas the homogeneous part $\boldsymbol{l}_h$ is independent of the choice of the origin. With the homogeneous coordinates $\mathbf{x}^e = [u, v, w]^\mathsf{T}$ for points and the homogeneous 3-vector for a

straight line **l** the incidence can be expressed by

$$\mathbf{x} \cdot \mathbf{l} = \mathbf{x}^\mathsf{T} \mathbf{l} = \mathbf{l}^\mathsf{T} \mathbf{x} = 0.$$

The covariance matrix $\mathbf{\Sigma}_{\mathrm{ll}}$ of the parameters $\underline{a}$, $\underline{b}$ and $\underline{c}$ of the straight line in general has rank 3 unless certain constraints are imposed on **l**. This is the reason why one must allow the factor λ to be chosen stochastic, in order to be able to achieve a rank 3 matrix $\mathbf{C}_{\mathrm{ll}}$ by error propagation from the Hessian parameters, which otherwise would only lead to a rank 2 covariance matrix, cf. the discussion in (Förstner, 2005).

The parameters of the Hessian normal form can be derived from the homogeneous coordinates by $\phi = \mathrm{atan2}\,(b, a)$ and $d = -c/\sqrt{a^2 + b^2}$. Again, the covariance matrix of the parameters results from variance propagation $\mathbf{\Sigma}_{hh} = \boldsymbol{J}(\boldsymbol{\mu}_{\mathrm{l}}) \mathbf{\Sigma}_{\mathrm{ll}} \boldsymbol{J}^\mathsf{T}(\boldsymbol{\mu}_{\mathrm{l}})$ with

$$\boldsymbol{J}(\mathbf{l}) = \begin{bmatrix} \dfrac{-b}{s^2} & \dfrac{a}{s^2} & 0 \\[2ex] \dfrac{ca}{s^3} & \dfrac{cb}{s^3} & \dfrac{-1}{s} \end{bmatrix}$$

and $s^2 = a^2 + b^2$. The covariance matrix in general has rank two.

For the inverse transformation we fix the arbitrary factor $\sqrt{a^2 + b^2} = 1$ and obtain

$$\mathbf{l} = \begin{bmatrix} a \\[1ex] b \\[1ex] c \end{bmatrix} = \begin{bmatrix} \cos(\phi) \\[1ex] \sin(\phi) \\[1ex] -d \end{bmatrix} .$$

The Jacobian and its null space is given by

$$\boldsymbol{J}(\boldsymbol{h}) = \frac{\partial \mathbf{l}}{\partial \boldsymbol{h}} = \begin{bmatrix} -\sin(\phi) & 0 \\ \cos(\phi) & 0 \\ 0 & -1 \end{bmatrix},$$

$$\mathcal{N}(\boldsymbol{J}(\boldsymbol{h})) = \begin{bmatrix} \cos(\phi) \\ \sin(\phi) \\ 0 \end{bmatrix}$$

with $\boldsymbol{h} = [\phi, d]^{\mathsf{T}}$. The null space of the resulting rank two covariance matrix $\Sigma_{\mathrm{ll}} = \boldsymbol{J}(\boldsymbol{\mu}_h)\Sigma_{hh}\boldsymbol{J}^{\mathsf{T}}(\boldsymbol{\mu}_h)$ is $[\boldsymbol{\mu}_{l_h}^{\mathsf{T}}, 0]^{\mathsf{T}}$.

3.2.2 Conic representation of a straight line.

A further representation of an uncertain line is the hyperbolic error band being the set of (normalized) confidence regions across the line of all points on the line, as plotted in Fig. 3. For points y with homogeneous coordinates $\mathbf{y} = [u, v, w]^{\mathsf{T}}$ holds $\mathbf{y}^{\mathsf{T}}\mathbf{C}_{\mathrm{ll}}\mathbf{y} = 0$ and thus we may represent the hyperbola as

$$\boxed{\ell: \quad \mathbf{C}_{\mathrm{ll}}}.$$

We use the possibility to represent a conic, here a hyperbola, by a 3×3-matrix. Moreover, one can show, that this definition of the hyperbola is identical to the envelope of all lines of the standard confidence ellipse, e.g. $\boldsymbol{h}^{\mathsf{T}}C_{hh}\boldsymbol{h} = 1$, of the line parameters.

Exploiting the principle of duality, cf. (Hartley and Zisserman, 2000) and (McGlone et al., 2004), and using Eq. 7 the standard confidence hyperbola for the uncertain line referring to $\mathbf{l}$ is given by

$$\mathbf{C}_{\mathrm{ll}} = \mathbf{\Sigma}_{\mathrm{ll}} - \mathbf{l}\mathbf{l}^{\mathsf{T}},$$

cf. (Ochoa and Belongie, 2006). Again this relation holds for general $\mathbf{\Sigma}_{\mathrm{ll}}$.

With the rotation angle and the translation (Eqn. 8 and 9) the motion matrix $\mathbf{M}$ can be computed (Eq. 10). The standard deviations σ_α and σ_q result from the eigenvalues of the normalized matrix $\mathbf{C}/C_{33}$ with $\mathbf{C} = (C_{ij}) = \mathbf{M}^{-\mathsf{T}}\mathbf{C}_{\mathrm{ll}}\mathbf{M}^{-1}$, namely $\sigma_q = \sqrt{\lambda_1}$ and $\sigma_\alpha = \sqrt{-\lambda_2}$. Note, that for hyperbolas the second eigenvalue is negative.

3.2.3 Normalization

Also here Euclidean and spherical normalization can be used. As the spherical normalization of lines is equivalent to points, we only give the Euclidean normalization and the corresponding representation of the uncertain line. Again, it may replace the general homogeneous representation.

Division of a homogeneous line vector by the norm of its homogeneous part yields the Euclidean representation of a straight line which is closely related to the Hessian normal form. The Euclidean normalized homogeneous representation of a line is

$$\mathit{l} : \quad \{\mathbf{l}^e, \mathbf{\Sigma}_{\mathrm{ll}}^e\}$$

with the line parameters

$$\mathbf{l}^e = \mathsf{N}_e(\mathbf{l}) = \frac{\mathbf{l}}{|\boldsymbol{l}_h|} = \frac{1}{\sqrt{a^2 + b^2}} \begin{bmatrix} a \\ b \\ c \end{bmatrix} = \begin{bmatrix} \cos(\phi) \\ \sin(\phi) \\ -d \end{bmatrix},$$

if $|\boldsymbol{l}_h| \neq 0$.

With the Jacobian

$$\boldsymbol{J}_e(\mathbf{l}) = \frac{\partial \mathsf{N}_e(\mathbf{l})}{\partial \mathbf{l}} = \frac{1}{|\boldsymbol{l}_h|} \begin{bmatrix} \boldsymbol{I}_2 - \frac{\boldsymbol{l}_h \boldsymbol{l}_h^\mathsf{T}}{|\boldsymbol{l}_h|^2} & \mathbf{0} \\ -\frac{l_0 \boldsymbol{l}_h^\mathsf{T}}{|\boldsymbol{l}_h|^2} & 1 \end{bmatrix}$$

we obtain the covariance matrix $\Sigma_{\mathrm{ll}}^e = \boldsymbol{J}_e(\boldsymbol{\mu}_{\mathrm{l}})\Sigma_{\mathrm{ll}}\boldsymbol{J}_e^\mathsf{T}(\boldsymbol{\mu}_{\mathrm{l}})$. Once again, the ambiguity in the sign of the result has no influence on the result of the variance propagation.

3.2.4 *Conditioning*

With the conditioning matrix for points (Eq. 13) the conditioned line representation is $\ell : \{\mathbf{T}_c^{-\mathsf{T}}\mathbf{l}, \quad \mathbf{T}_c^{-\mathsf{T}}\Sigma_{\mathrm{ll}}\mathbf{T}_c^{-1}\}$. Observe, that the parameters x_c, y_c and s in $\mathbf{T}_c$ cannot easily be derived from given lines only.

4 Construction of Uncertain 2D Points and Straight Lines

Join and intersection of points and lines are basic, and mutually dual, operations. Uncertainty propagation is easy due to the bi-linearity of the relations. These constructions are needed for the derivation of the representations for uncertain straight

28

line segments given in the next section.

4.1 Straight line from two points

A straight line l is constructed by the join of two points x and y realized by the cross product

$$\mathbf{l} = \mathbf{x} \times \mathbf{y} = \mathbf{S}_x \mathbf{y} = -\mathbf{S}_y \mathbf{x}. \tag{18}$$

In general the two points are uncertain and correlated. Starting from the uncertain point pair

$$\{\mathbf{p}, \Sigma_{pp}\} = \left\{ \begin{bmatrix} \mathbf{x} \\ \\ \mathbf{y} \end{bmatrix}, \begin{bmatrix} \Sigma_{xx} & \Sigma_{xy} \\ \\ \Sigma_{yx} & \Sigma_{yy} \end{bmatrix} \right\} \tag{19}$$

and the Jacobian $\boldsymbol{J}(\mathbf{p}) = \partial \mathbf{l}/\partial \mathbf{p} = [-\mathbf{S}(\mathbf{y}), \mathbf{S}(\mathbf{x})]$ we can derive the covariance matrix $\Sigma_{ll} = \boldsymbol{J}(\boldsymbol{\mu}_p)\Sigma_{pp}\boldsymbol{J}^{\mathsf{T}}(\boldsymbol{\mu}_p)$. In case the two points are uncorrelated we obtain

$$\Sigma_{ll} = \mathbf{S}(\boldsymbol{\mu}_y)\Sigma_{xx}\mathbf{S}^{\mathsf{T}}(\boldsymbol{\mu}_y) + \mathbf{S}(\boldsymbol{\mu}_x)\Sigma_{yy}\mathbf{S}^{\mathsf{T}}(\boldsymbol{\mu}_x).$$

The covariance matrix Σ_{ll} has *full* rank, cf. (McGlone et al., 2004), Subsection 2.3.5.2. In order to be able to interpret the covariance matrix one must allow for uncertain scale factors when deriving homogeneous coordinates from Euclidean coordinates. The scale factor here is uncertain, as the length of the cross product depends on two uncertain vectors, however, the length of the vector $\mathbf{l}$ is of no concern.

4.2   Point from two straight lines

A point χ results from the intersection of two straight lines l and m realized by the cross product

$$\mathbf{x} = \mathbf{l} \times \mathbf{m} = \mathbf{S}_l \mathbf{m} = -\mathbf{S}_m \mathbf{l}.$$

Starting from the uncertain line pair $\{\mathbf{r}, \Sigma_{rr}\}$, i.e., $\mathbf{r} = [\mathbf{l}^\mathsf{T}, \mathbf{m}^\mathsf{T}]^\mathsf{T}$ and the Jacobian $J(\mathbf{r}) = \partial \mathbf{x}/\partial \mathbf{r} = [-\mathbf{S}(\mathbf{m}), \mathbf{S}(\mathbf{l})]$ we can derive the covariance matrix $\Sigma_{xx} = J(\boldsymbol{\mu}_r)\Sigma_{rr}J^\mathsf{T}(\boldsymbol{\mu}_r)$ which also in general has full rank.

5   Representation of Uncertain Straight Line Segments

Straight line segments play a central role in image analysis. They can only be represented as aggregates of points or lines. No homogeneous representation is known to the authors.

5.1   Representing line segments using points pairs

The most natural representation for a straight line segment is $s : \{\chi, y\}$ based on its two end points χ and y. In principle any representation described in Section 3 is applicable. In the Euclidean case this means, that a line segment is represented as

$$\boxed{s : \quad \{\boldsymbol{p}; \Sigma_{pp}\}}$$

with $\boldsymbol{p} = [x_1, x_2, y_1, y_2]^\mathsf{T}$ and the corresponding covariance matrix which in general has rank 4. This amounts in fourteen parameters for an uncertain line segment

in the plane. Some of those parameters may be assumed zero, if for example the end points are assumed to be uncorrelated. Note also, that the line segment has a direction defined as pointing from χ to y.

In homogeneous coordinates, the line segment is represented using its two end points in homogeneous representation as

$$s: \quad \{\mathbf{p}; \Sigma_{\mathrm{pp}}\}$$

with

$$\mathbf{p} = \begin{bmatrix} \mathbf{x} \\ \\ \mathbf{y} \end{bmatrix} \quad \text{and} \quad \Sigma_{\mathrm{pp}} = \begin{bmatrix} \Sigma_{\mathrm{xx}} & \Sigma_{\mathrm{xy}} \\ \\ \Sigma_{\mathrm{yx}} & \Sigma_{\mathrm{yy}} \end{bmatrix}.$$

This covariance matrix may have rank four, five or six, with the null space depending on the normalization as described above. Observe, we have written the line segment $\mathbf{p}$ with an upright letter to indicate the two points being represented with homogeneous coordinates; however, the complete 6-vector is *not* a homogeneous quantity, as the two parts $\mathbf{x}$ and $\mathbf{y}$ may be scaled independently.

5.2 *Representing line segments using line triplets*

Another useful representation for line segments uses a line triplet namely the straight line l joining its end points and the two delimiting lines m and n going perpendicularly through the end points (see Fig. 4), thus $s : \{l, m, n\}$. Again any representation from Section 3 is applicable. Using a homogeneous representation, this means
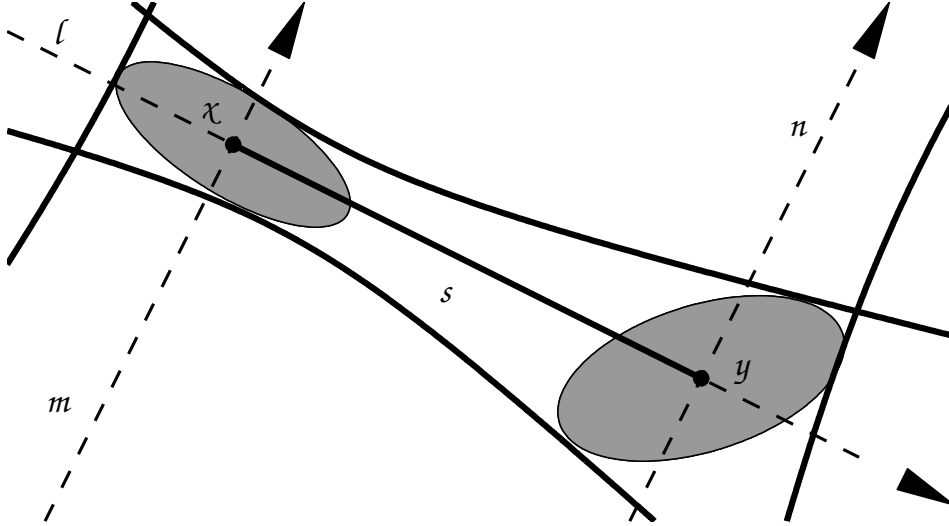
31

Fig. 4. shows a straight line segment s delimited by two straight lines m and n going perpendicularly through the end points x and y. The corresponding error region of s results from the intersection of the hyperbolic error bands of the straight line l and the delimiting lines m and n.

that a line segment is represented as line triplet

$$s: \quad \{\mathbf{t}; \Sigma_{tt}\}$$

with

$$\mathbf{t} = \begin{bmatrix} \mathbf{l} \\ \mathbf{m} \\ \mathbf{n} \end{bmatrix} \quad \text{and} \quad \Sigma_{tt} = \begin{bmatrix} \Sigma_{ll} & \Sigma_{lm} & \Sigma_{ln} \\ \Sigma_{ml} & \Sigma_{mm} & \Sigma_{mn} \\ \Sigma_{nl} & \Sigma_{nm} & \Sigma_{nn} \end{bmatrix}.$$

Not every such 9-vector with corresponding covariance matrix is actually a line segment, because of the perpendicularity constraint. In the homogeneous representation the latter is easily formulated by stating, that the above represents a line segment if and only if the two conditions

32

$$\mathbf{l}^\mathsf{T}\mathbf{C}_\infty^*\mathbf{m} = 0 \qquad \text{and} \qquad \mathbf{l}^\mathsf{T}\mathbf{C}_\infty^*\mathbf{n} = 0 \tag{20}$$

hold, with the dual conic $\mathbf{C}_\infty^* = \mathrm{Diag}\,(1,1,0)$ of the circular points, cf. (Hartley and Zisserman, 2000, p. 33f). The two conditions imply also a specific null space of the covariance matrix. Since $\mathbf{C}_\infty^*\mathbf{m} = \lambda\mathbf{C}_\infty^*\mathbf{n}$ are linearly dependent, the null space induced by the perpendicularity constraints is two-dimensional reducing the rank of Σ_{tt} by two. Therefore, the rank of Σ_{tt} may be four, five, or six with the extra null space depending on the normalization of the three lines. As expected, this agrees exactly with the degrees of freedom for the representation using points.

Note also, that end points at infinity are possible with this representation, then $\mathbf{m}$ or $\mathbf{n}$ are the line at infinity $[0,0,1]^\mathsf{T}$, which always fulfills the orthogonality constraints.

It is often convenient to fix the orientation of the two lines m and n: the directions of the lines m and n should be parallel to the normal of l. These constraints can be written as

$$\mathbf{l}^\mathsf{T}\mathbf{C}_\infty^*\mathbf{R}_\perp\mathbf{m} > 0 \qquad \text{and} \qquad \mathbf{l}^\mathsf{T}\mathbf{C}_\infty^*\mathbf{R}_\perp\mathbf{n} > 0$$

with the rotation matrix

$$\mathbf{R}_\perp = \begin{bmatrix} 0 & 1 & 0 \\ -1 & 0 & 0 \\ 0 & 0 & 1 \end{bmatrix} \tag{21}$$

rotating the normal of a line into the direction of the line.

In the following we derive the conversion from the point pairs to the line triplets representation. Given a line segment in point pair representation (Eq. 19), the three elements of the line triplet can be expressed as

$$
\mathbf{t} = \begin{bmatrix} \mathbf{l} \\ \mathbf{m} \\ \mathbf{n} \end{bmatrix} = \begin{bmatrix} \mathbf{S}_x \mathbf{y} \\ \mathrm{sgn}(y_h) \mathbf{U}_x \mathbf{y} \\ -\mathrm{sgn}(x_h) \mathbf{U}_y \mathbf{x} \end{bmatrix}
$$

with the matrices $\mathbf{U}_x = \mathbf{S}_x \mathbf{C}_\infty^* \mathbf{S}_x$ and $\mathbf{U}_y = \mathbf{S}_y \mathbf{C}_\infty^* \mathbf{S}_y$ (cf. Section 5.2).

The $\mathrm{sgn}(\cdot)$-factors are necessary to ensure the correct orientation of the lines $\mathbf{m}$ and $\mathbf{n}$. While the expression for $\mathbf{l}$ is bilinear in $\mathbf{x}$ and $\mathbf{y}$, the expression for the bounding lines $\mathbf{m}$ and $\mathbf{n}$ are quadratic in $\mathbf{x}$ and $\mathbf{y}$.

First we prove these relations, then we give the Jacobian $\boldsymbol{J}_{\mathrm{tp}}(\mathbf{p}) = \partial \mathbf{t}/\partial \mathbf{p}$.

The directed line l from x to y is constructed by Eq. 18. Therefore, we have the following Jacobians evaluated at $\mathbf{p} = [\mathbf{x}^\mathsf{T}, \mathbf{y}^\mathsf{T}]^\mathsf{T}$

$$
\boldsymbol{J}_{\mathrm{lx}}(\mathbf{p}) = -\mathbf{S}(\mathbf{y}) \qquad \text{and} \qquad \boldsymbol{J}_{\mathrm{ly}}(\mathbf{p}) = \mathbf{S}(\mathbf{x}).
$$

The bounding line m through x perpendicular to l is constructed as follows: from Eq. 20 follows directly, that the point $\mathbf{x}' = \mathbf{C}_\infty^* \mathbf{l}$ must sit on m. Therefore $\mathbf{m}$ is obtained by connecting the two points $\mathbf{x}$ and $\mathbf{x}'$. Taking care of the sign as described above, this yields

$$
\mathbf{m} = \mathrm{sgn}(y_h) \mathbf{S}_x \mathbf{x}' = \mathrm{sgn}(y_h) \mathbf{S}_x \mathbf{C}_\infty^* \mathbf{S}_x \mathbf{y} = \mathrm{sgn}(y_h) \mathbf{U}_x \mathbf{y}
$$

34

with

$$\mathbf{U}_\mathrm{x} = \mathbf{S}_\mathrm{x} \mathbf{C}_\infty^* \mathbf{S}_\mathrm{x} = \begin{bmatrix} -x_h^2 \boldsymbol{I}_2 & x_h \boldsymbol{x}_0 \\[2em] x_h \boldsymbol{x}_0^\mathsf{T} & -\boldsymbol{x}_0^\mathsf{T} \boldsymbol{x}_0 \end{bmatrix}.$$

This expression is linear in $\mathbf{y}$ but not in $\mathbf{x}$. Therefore, the Jacobian is

$$\boldsymbol{J}_\mathrm{mx}(\mathbf{p}) = \mathrm{sgn}(y_h) \begin{bmatrix} x_h y_h \boldsymbol{I}_2 & y_h \boldsymbol{x}_0 - 2x_h \boldsymbol{y}_0 \\[2em] x_h \boldsymbol{y}_0^\mathsf{T} - 2y_h \boldsymbol{x}_0^\mathsf{T} & \boldsymbol{x}_0^\mathsf{T} \boldsymbol{y}_0 \end{bmatrix}$$

for variance propagation. The Jacobian with respect to $\mathbf{y}$ is given by $\boldsymbol{J}_\mathrm{my}(\mathbf{p}) = \mathrm{sgn}(y_h)\mathbf{U}(\mathbf{x})$.

The construction of the second delimiting straight line n is done completely analogous to the line m by swapping the roles of $\mathbf{x}$ and $\mathbf{y}$. We have $\mathbf{n} = -\mathrm{sgn}(x_h)\mathbf{U}_\mathrm{y}\mathbf{x}$. Again this is linear in $\mathbf{x}$ but not in $\mathbf{y}$. The Jacobians are

$$\boldsymbol{J}_\mathrm{nx}(\mathbf{p}) = \frac{\partial \mathbf{n}}{\partial \mathbf{x}} = -\mathrm{sgn}(\mu_{x_h})\mathbf{U}(\mathbf{y})$$

and

$$\boldsymbol{J}_\mathrm{ny}(\mathbf{p}) = \mathrm{sgn}(x_h) \begin{bmatrix} x_h y_h \boldsymbol{I}_2 & x_h \boldsymbol{y}_0 - 2y_h \boldsymbol{x}_0 \\[2em] y_h \boldsymbol{x}_0^\mathsf{T} - 2x_h \boldsymbol{y}_0^\mathsf{T} & \boldsymbol{y}_0^\mathsf{T} \boldsymbol{x}_0 \end{bmatrix}.$$

35

Therefore, the complete Jacobian is

$$
\boldsymbol{J}_{\mathrm{tp}}(\mathbf{p}) = \frac{\partial \mathbf{t}}{\partial \mathbf{p}} =
\begin{bmatrix}
\boldsymbol{J}_{\mathrm{lx}} & \boldsymbol{J}_{\mathrm{ly}} \\
\boldsymbol{J}_{\mathrm{mx}} & \boldsymbol{J}_{\mathrm{my}} \\
\boldsymbol{J}_{\mathrm{nx}} & \boldsymbol{J}_{\mathrm{ny}}
\end{bmatrix}
$$

yielding the covariance matrix $\Sigma_{\mathrm{tt}} = \boldsymbol{J}_{\mathrm{tp}}(\boldsymbol{\mu}_{\mathrm{p}}) \Sigma_{\mathrm{pp}} \boldsymbol{J}_{\mathrm{tp}}^{\mathsf{T}}(\boldsymbol{\mu}_{\mathrm{p}})$.

Conversely, given a line segment with homogeneous line representation, the corresponding line segment in homogeneous point representation is obtained by intersecting the line ℓ with the lines m and n to obtain the two end points. The relation is bilinear yielding

$$
\mathbf{p} =
\begin{bmatrix}
\mathbf{x} \\
\mathbf{y}
\end{bmatrix}
= \boldsymbol{J}_{\mathrm{pt}}(\mathbf{t}) \quad \mathbf{t} =
\begin{bmatrix}
-\mathbf{S}_{\mathrm{m}} & \mathbf{S}_{\mathrm{l}} & O \\
-\mathbf{S}_{\mathrm{n}} & O & \mathbf{S}_{\mathrm{l}}
\end{bmatrix}
\begin{bmatrix}
\mathbf{l} \\
\mathbf{m} \\
\mathbf{n}
\end{bmatrix}
$$

leading to the covariance matrix $\Sigma_{\mathrm{pp}} = \boldsymbol{J}_{\mathrm{pt}}(\boldsymbol{\mu}_{\mathrm{t}}) \Sigma_{\mathrm{tt}} \boldsymbol{J}_{\mathrm{pt}}^{\mathsf{T}}(\boldsymbol{\mu}_{\mathrm{t}})$.

5.3   *Centroid representation of the line segment*

A third commonly used representation describes a line segment by the coordinates of its centre $\boldsymbol{x_0}$, its direction α and its length ℓ leading to

$$
\boxed{s: \quad \{\boldsymbol{c}, \Sigma_{cc}\}}
$$

with $\boldsymbol{c} = [\boldsymbol{x}_0, \alpha, \ell]^\mathsf{T}$ and the corresponding covariance matrix Σ_{cc} — again yielding a total maximum of fourteen parameters, some of them possibly being zero under certain independence assumptions.

The centroid representation is Euclidean. Therefore, we give the conversion to and from Euclidean point pairs, as the conversion from homogeneous to Euclidean points is always possible in case of real, thus non-ideal points.

Given a line segment in Euclidean point representation the coordinates of the center are $\boldsymbol{x}_0 = (\boldsymbol{x} + \boldsymbol{y})/2$, the angle with the x-axis is $\alpha = \arctan(y_2 - x_2)/(y_1 - x_1)$, and the length is $\ell = \sqrt{(\boldsymbol{y} - \boldsymbol{x})^\mathsf{T}(\boldsymbol{y} - \boldsymbol{x})}$. The covariance is obtained as $\Sigma_{cc} = \boldsymbol{J}_{cp}(\boldsymbol{\mu}_p)\Sigma_{pp}\boldsymbol{J}_{cp}(\boldsymbol{\mu}_p)^\mathsf{T}$ with the Jacobian $\boldsymbol{J}_{cp} = \partial\boldsymbol{c}/\partial\boldsymbol{p}$ being easily derived.

Given a line segment in centroid representation the Euclidean coordinates of the end points are obtained as

$$\boldsymbol{x} = \boldsymbol{x}_0 - \frac{\ell}{2}\begin{bmatrix}\sin(\alpha) \\ \cos(\alpha)\end{bmatrix}, \quad \boldsymbol{y} = \boldsymbol{x}_0 + \frac{\ell}{2}\begin{bmatrix}\sin(\alpha) \\ \cos(\alpha)\end{bmatrix}$$

and the covariance matrix of the Euclidean point pair is $\Sigma_{pp} = \boldsymbol{J}_{pc}\Sigma_{cc}\boldsymbol{J}_{pc}^\mathsf{T}$ with the Jacobian $\boldsymbol{J}_{pc} = \partial\boldsymbol{p}/\partial\boldsymbol{c}$ being easily derived.

6 Statistical Testing

A key advantage of representing entities together with their uncertainties is the possibility of statistical testing. This eliminates the necessity of specifying non-interpretable thresholds: only a single confidence probability is required.

Statistical tests can be used in our context

- as a sieve to eliminate relations which are likely not to hold, but also,

- to derive conjectures.

In the following specific test statistics and hypothesis for various geometric relations between the entities are given. We follow the classical testing procedures according to Neyman and Pearson (Neyman and Pearson, 1933), as we have no prior probabilites for alternative hypotheses, and therefore in general cannot apply Bayesian testing, cf. (Jeffreys, 1961).

6.1 Testing Relations Between Points and Straight Lines

We discuss the testing of the relations between points and straight lines based on the representations derived in the preceding sections, cf. Fig. 5.
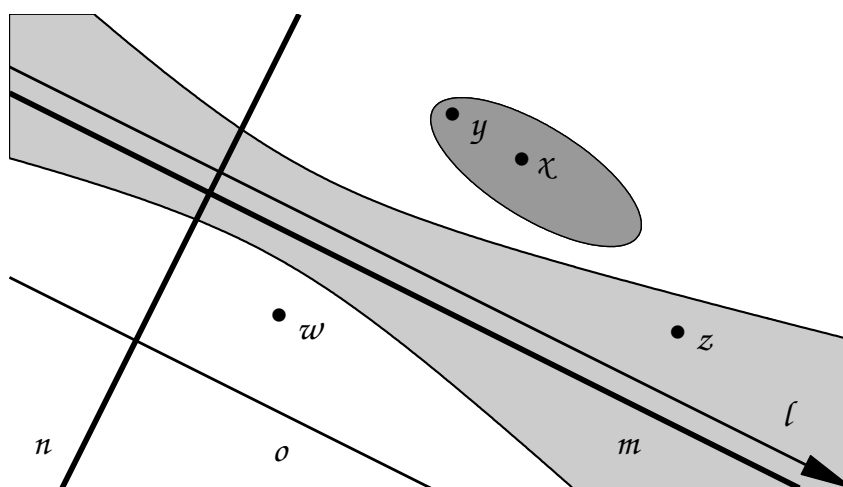
Fig. 5. Different relations between points and straight lines. The point z is incident to the line l, because it is within the confidence region of l. The point x is left of the line l and the point w is right of the line l. The two uncertain points x and y are considered equal as are the two uncertain lines l and m. The lines l and n are perpendicular and the lines l and o are parallel.

6.1.1 Incidence of points and straight lines

We test the null-hypothesis $H_0 : x \in l$ that a point x lies on a line l. The test statistic is

$$\underline{z} = \underline{d}/\sigma_d \sim N(0, 1)$$

with

$$\underline{d}(x, l) = \mathrm{sgn}(x_h)\underline{\mathbf{x}}^{\mathsf{T}}\underline{\mathbf{l}} = \mathrm{sgn}(x_h)\underline{\mathbf{l}}^{\mathsf{T}}\underline{\mathbf{x}}$$

and its variance

$$\sigma_d^2 = \boldsymbol{\mu}_{\mathrm{x}}^{\mathsf{T}}\Sigma_{\mathrm{ll}}\boldsymbol{\mu}_{\mathrm{x}} + \boldsymbol{\mu}_{\mathrm{l}}^{\mathsf{T}}\Sigma_{\mathrm{xx}}\boldsymbol{\mu}_{\mathrm{l}}.$$

Observe, we in general do not have access to the means $\boldsymbol{\mu}_{\mathrm{x}}$ and $\boldsymbol{\mu}_{\mathrm{l}}$. Therefore, one can approximate the means by the sample value $\mathbf{x}$ and $\mathbf{l}$. In case the hypothesis H_0 is not rejected, the effect of this approximation is of second order. In case H_0 is rejected, the effect can be large, cf. (Heuel, 2004).

This test statistic T shows, that a point lies on the *positive* or *left* side of the line, thus the same side as the normal of the line,

$$x \in^+ l \quad \text{if} \quad d(x, l) > 0$$

and on the *negative* or *right* side of the line, thus the opposite side as the normal of the line,

$$x \in^- l \quad \text{if} \quad d(x, l) < 0.$$

We thus have three alternatives:

(1) $H_{a_1} : \chi \in^+ \ell$: We test H_0 against the alternative that the point χ lies on the left side of ℓ. The corresponding rejection region is $\mathcal{R}_1 : \ z > \phi_S$ with the S-quantile ϕ_S of the normal distribution. Thus the probability of rejecting H_0, in case it actually is true, is S. If this test is not rejected we may conjecture $\chi \in^- \ell$ or H_0. Observe, this conjecture is the negation of the alternative hypothesis.

(2) $H_{a_2} : \chi \in^- \ell$: We test H_0 against the alternative that the point χ sits on the right side of ℓ. The corresponding rejection region is $\mathcal{R}_2 : \ z < -\phi_S$. If this test is not rejected we may conjecture $\chi \in^+ \ell$ or H_0.

(3) $H_{a_3} : \chi \notin \ell$: We test H_0 against the alternative that the point does not lie on the line. The corresponding rejection region is $\mathcal{R}_3 : \ |z| > \phi_S$. If this test is not rejected we may conjecture $\chi \in \ell$. This test is logically equivalent to the union of the first and the second test, as $\chi \notin \ell = (\chi \in^+ \ell) \wedge (\chi \in^- \ell)$. However, using the same significance levels $S_{1,2}$ for the one-sided tests and S_3 for the two-sided tests leads to different acceptance regions. The acceptance regions are only identical if $1 - S_3 = 2(1 - S_{1,2})$ is chosen.

6.1.2 *Identity of two points and two lines*

We test the null-hypothesis $H_0 : \ \chi = y$ that two points χ and y are identical. The test statistic is

$$\underline{T} = \underline{\mathbf{d}}^\mathsf{T} \Sigma_{\mathrm{dd}}^{-1} \underline{\mathbf{d}} \sim \chi_2^2$$

with the 2-vector (for $\overline{\mathbf{S}}_\mathrm{x}$ cf. below)

$$\underline{\mathbf{d}}(\chi, y) = \overline{\mathbf{S}}_\mathrm{x}\underline{y} = -\overline{\mathbf{S}}_\mathrm{y}\underline{\mathbf{x}}$$

and the covariance matrix

$$\Sigma_{\mathrm{dd}} = \overline{\mathbf{S}}(\boldsymbol{\mu}_{\mathrm{x}})\Sigma_{\mathrm{yy}}\overline{\mathbf{S}}^{\mathsf{T}}(\boldsymbol{\mu}_{\mathrm{x}}) + \overline{\mathbf{S}}(\boldsymbol{\mu}_{\mathrm{y}})\Sigma_{\mathrm{xx}}\overline{\mathbf{S}}^{\mathsf{T}}(\boldsymbol{\mu}_{\mathrm{y}}).$$

This test statistic results from Eq. 18 as in case the two points are identical the joining line is indefinite and thus $\mathbf{l} = \mathbf{S}(\mathbf{x})\mathbf{y} = -\mathbf{S}(\mathbf{y})\mathbf{x} = \mathbf{0}$. As the skew symmetric matrices have rank two, *two rows must be selected* to avoid linear dependent conditions. For the sake of numerical stability it is reasonable to select the two rows, which contain the elements with maximum absolute values. We denote this reduced matrices as $\overline{\mathbf{S}}_{\mathrm{x}}$. In case the points are not at infinity one can select the first two rows, yielding

$$\overline{\mathbf{S}}_{\mathrm{x}} = \begin{bmatrix} 0 & -x_3 & x_2 \\ x_3 & 0 & -x_1 \end{bmatrix}.$$

If for two points x and y we have $\underline{T} > \chi^2_{2,S}$ with the S-quantile of the χ^2_2-distribution, the null-hypothesis $H_0 : \quad x = y$ will be rejected in favour of the alternative hypothesis $H_a : \quad x \neq y$. If the test is not rejected, we may conjecture $x = y$.

For duality reasons the same reasoning applies for testing the equality of straight lines l and m, using the fact, that two lines define no intersection point, i.e., are identical, if and only if

$$\mathbf{d}(\mathbf{l}, \mathbf{m}) = \overline{\mathbf{S}}_{\mathrm{l}}\mathbf{m} = -\overline{\mathbf{S}}_{\mathrm{m}}\mathbf{l} = \mathbf{0}. \tag{22}$$

6.1.3 Orthogonality and parallelism of straight lines

We test the null-hypothesis

$$H_0: \quad \ell \perp m$$

that two lines ℓ and m are orthogonal [2]. The test statistic is

$$\underline{z} = \underline{d}^\perp / \sigma_{d^\perp} \sim N(0,1)$$

with

$$d^\perp(\mathbf{l}, \mathbf{m}) = \mathbf{l}^\mathsf{T} \mathbf{C}_\infty^* \mathbf{m} = \mathbf{m}^\mathsf{T} \mathbf{C}_\infty^* \mathbf{l} = 0$$

and its variance

$$\sigma_{d^\perp}^2 = \boldsymbol{\mu}_\mathrm{l}^\mathsf{T} \mathbf{C}_\infty^* \boldsymbol{\Sigma}_\mathrm{mm} \mathbf{C}_\infty^* \boldsymbol{\mu}_\mathrm{l} + \boldsymbol{\mu}_\mathrm{m}^\mathsf{T} \mathbf{C}_\infty^* \boldsymbol{\Sigma}_\mathrm{ll} \mathbf{C}_\infty^* \boldsymbol{\mu}_\mathrm{m}.$$

If the test statistic for two lines is not rejected one may conjecture $\ell \perp m$.

In a similar manner we may test the hypothesis $H_0: \quad \ell \| m$ versus the alternative $H_a: \quad \ell \nparallel m$. The test statistic is

$$\underline{z} = \underline{d}^{\|} / \sigma_d^{\|} \sim N(0,1)$$

with

$$d^{\|}(\ell, m) = \mathbf{l}^\mathsf{T} \mathbf{C}_\infty^* \mathbf{R}_\perp \mathbf{m} = \mathbf{m}^\mathsf{T} \mathbf{R}_\perp{}^\mathsf{T} \mathbf{C}_\infty^* \mathbf{l}$$

---

[2] Here m is a line independently observed from ℓ and is not to be confused with the bounding line of a line segment.

and its variance

$$\sigma_{d\parallel}^2 = \mathbf{\mu}_l^\mathsf{T} \mathbf{C}_\infty^* \mathbf{R}_\perp \mathbf{\Sigma}_{\mathrm{mm}} \mathbf{R}_\perp^\mathsf{T} \mathbf{C}_\infty^* \mathbf{\mu}_l$$
$$+ \mathbf{\mu}_\mathrm{m}^\mathsf{T} \mathbf{R}_\perp^\mathsf{T} \mathbf{C}_\infty^* \mathbf{\Sigma}_{\mathrm{ll}} \mathbf{C}_\infty^* \mathbf{R}_\perp \mathbf{\mu}_\mathrm{m}$$

with the rotation matrix in Eq. 21. In case the test statistic for two lines is not rejected we may conjecture $l \parallel m$.

6.2   Testing Straight Line Segments

In Section 5 it was shown, how line segments can be represented as aggregates of either homogeneous points or homogeneous lines. Therefore, also the tests are combinations of the tests presented in the previous sections, cf. Fig. 6.

6.2.1   Incidence of points and line segments

For the incidence a point χ and a line segment $s = (l, m, n)$ we have the equivalence

$$\chi \in s \iff (\chi \in l) \wedge (\chi \in^+ m) \wedge (\chi \in^- n)$$

where $\wedge$ denotes the logical "and". Thus testing, whether a point sits on a line segment is a composition of three elementary tests.

6.2.2   Intersection of two line segments

Checking if two line segments s and t intersect, is a little more involved. It requires to use two representations of a straight line segment at the same time

$$s = (\chi_s, y_s) = (l_s, m_s, n_s)$$
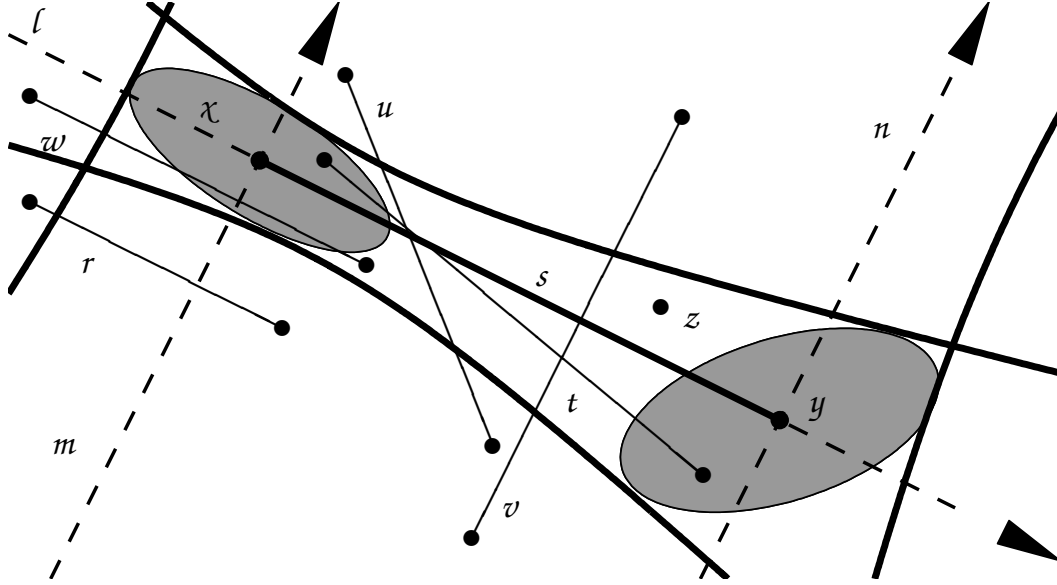
Fig. 6. Different relations involving straight line segments. The point z is incident to the line segment s, because it is incident to the line ℓ and between the two delimiting lines m and n. The line segment t is equal to the line segment s, because their end points are identical. The line segments s and w overlap, because the two lines are identical and the delimiting line m is between the two end points of w. The line segments s and r are parallel and overlap, because the line m is between the end points of r and the two lines are parallel. The line segment u intersects the line segment s and vice versa, because their end points are on the two different sides of the respective other line segment. The line segment s and v overlap and are orthogonal, because in addition to intersection the two lines are orthogonal.

$$t = (x_t, y_t) = (\ell_t, m_t, n_t)$$

which fortunately are easily convertible as shown in Section 5. The idea is, that two line segments intersect, if and only if the end points of the first segment lie on different sides of the line defined by the second segment and vice versa, cf. (Cormen et al., 1990, p. 889f). One has the equivalence relation

$$\text{intersect}(s, t) \Longleftrightarrow$$
$$\left(\left((x_s \in^- \ell_t) \wedge (y_s \in^+ \ell_t) \right) \vee \left((x_s \in^+ \ell_t) \wedge (y_s \in^- \ell_t) \right) \right)$$
$$\wedge \left(\left((x_t \in^- \ell_s) \wedge (y_t \in^+ \ell_s) \right) \vee \left((x_t \in^+ \ell_s) \wedge (y_t \in^- \ell_s) \right) \right)$$

where $\vee$ denotes the logical "or" operation. Thus between four and eight tests are required.

Combining statistical tests with the various representations given one is able to formulate many more useful hypotheses. Among them are the following:

(1) *Collinearity of line segments with overlap* requires up to five tests

(2) *Equality of line segments* requires up to four tests

(3) *Orthogonality of line segments with overlap* requires up to five tests

(4) *Parallelism of line segments with overlap* also requires up to five tests

Please observe the simple transfer of the deterministic tests to the statistical tests. Other tests may be set up similarly.

7   Estimation of Geometric Entities from Uncertain Observations

This last section deals with the statistical estimation of atomic or composed entities from observed atomic or composed uncertain geometric entities.

Well known estimation techniques in geometric computation (e.g. Chojnacki et al., 2001; Kanatani, 1994; Matei and Meer, 2000) usually only deal with single homogeneous vectors, such as points or transformations. These estimation techniques, such as algebraic minimization, total least squares, renormalization, or heteroscedastic regression cannot easily be generalized to the estimation of multiple homogeneous entities with multiple constraints, which is necessary for composed geometric entities such as straight line segments.

The set up proposed in the following is much more general, as it can handle multiple homogeneous vectors and multiple constraints. Yet, this advantage is balanced by

45

the need for approximate values for the unknown parameters.

The motivation behind the proposed estimation scheme is to allow the direct use of geometric constraints using homogeneous representations for both, observed as well as estimated entities. These constraints either between observed and unknown entities or among unknown parameters directly define the basic equations for a statistically optimal estimation scheme. For numerical reasons conditioning of the unknown entities is required, e.g., centering and scaling, using the conditioning matrix $\mathbf{T}_c$, cf. Eq. 13 in Section 2.2.4.

In the following a general estimation model and the corresponding iterative parameter estimation procedure will be derived, which is suitable for handling uncertain projective entities. It is based on the so-called Gauß-Helmert-model (Helmert, 1872), cf. (Mikhail, 1976; Heuel, 2004; McGlone et al., 2004), which employs constraints between observed and unknown parameters.

7.1 General Adjustment Model with Constraints

The model consists of a functional model for the unknown parameters and the observations, a stochastic model for the observations, an optimization criterion, and an iterative estimation procedure for non-linear problems.

7.1.1 Mathematical model

Functional model. We introduce three types of constraints for the true observations $\widetilde{l}$ and the true unknown parameters $\widetilde{p}$: conditions $g(\widetilde{l}, \widetilde{p}) = 0$ for the observations and parameters, constraints $k(\widetilde{l}) = 0$ for the observations, and restrictions $h(\widetilde{p}) = 0$ for the parameters.

46

The error-free observations $\widetilde{l}$ are related to the observations l by $\widetilde{l} = l + \widetilde{v}$, where the true corrections $\widetilde{v}$ are unknown. Since the true values remain unknown they are replaced by their estimates $\widehat{p}$, $\widehat{l}$ and $\widehat{v}$ in the following. The estimated corrections are negative residuals. Thus, together we have the three constraints

$$g(\widetilde{l}, \widetilde{p}) = 0, \quad h(\widetilde{p}) = 0, \quad \text{and} \quad k(\widetilde{l}) = 0.$$

Stochastic model. An initial covariance matrix $\Sigma_{ll}^{(0)}$ of the observations is assumed to be known which subsumes the statistical properties of the observations. Thus, l is assumed to be normally distributed $l \sim N(\widetilde{l}, \Sigma_{ll})$. The matrix is assumed to be related to the true covariance matrix Σ_{ll} by

$$\Sigma_{ll} = \sigma_0^2 \Sigma_{ll}^{(0)}$$

with the possibly unknown variance factor σ_0^2 (Koch, 1999). This factor can be estimated from the estimated corrections $\widehat{v}$.

This model is more general than the well known estimation techniques in two respects:

(1) It makes the *simultaneous estimation of more than one geometric entity* possible.

The *common algebraic optimizers* including their statistically rigorous variants reduce the estimation to an eigenvalue problem, possibly generalized or iterative. Thus only one quadratic constraint may directly be included. Therefore, only single geometric entities may be estimated. Also, two or more constraints cannot be introduced, preventing the simultaneous estimation of multiple entities or entities with two or more constraints, such as the fundamental

47

matrix.

(2) It allows the *consistent handling of arbitrary covariance matrices for the observed and the estimated entities.*

This can be a big advantage. An example is the estimation of the mean $\mathbf{m}$ of two points x_1 and x_2 (cf. Fig. 7). Assume they are given as homogeneous vectors $\underline{\mathbf{x}}_1 = [\underline{x}_1, \underline{y}_1, 1]^\mathsf{T}$ and $\underline{\mathbf{x}}_2 = [\underline{x}_2, \underline{y}_2, 1]^\mathsf{T}$ with uncertain Euclidean coordinates, thus singular covariance matrices $\Sigma_{\mathrm{x}_i \mathrm{x}_i}$ of the form of Eq. 4 and the estimated mean should be spherically normalized, thus $|\widehat{\mathbf{m}}|^2 - 1 = 0$ should hold. When minimizing $\Omega(\mathbf{m}) = \frac{1}{2}\sum_i (\mathbf{x}_i - \mathbf{m})^\mathsf{T} \Sigma_{\mathrm{x}_i \mathrm{x}_i}^- (\mathbf{x}_i - \mathbf{m})$ under the given constraints one needs to decide on the choice of the generalized inverse. Choosing the pseudo inverse would lead to

$$
\Sigma_{\mathrm{x}_i \mathrm{x}_i}^+ = \begin{bmatrix} \Sigma_{x_i x_i}^{-1} & \mathbf{0} \\ \\ \mathbf{0}^\mathsf{T} & 0 \end{bmatrix}.
$$

This inverse covariance matrix can be represented as an infinitely elongated, cylindrical confidence ellipsoid in (u, v, w)-space, with the infinitely long axis being parallel to the w axis. Yet, this would allow the homogeneous part of $\mathbf{x}_i$ to vary arbitrarily and in case the point lies outside the unit circle it would lead to extremely high values of Ω.

The reason for this situation is the inconsistency between the different constraints. Therefore, it is necessary that *the explicit constraints, e.g., for normalizing the result, and the implicit constraints, i.e., those contained in the uncertainty matrices Σ^-, are consistent.* This can be achieved under the following conditions (cf. Fig. 8):

(a) Normalize the given entities, say $\mathbf{x}$, spherically, leading to, say $\mathbf{x}^s$, cf. Eq. 12. Then the null space of their covariance matrix $\Sigma_{x^s x^s} = \boldsymbol{J}_s(\mathbf{x})\Sigma_{xx}\boldsymbol{J}_s^\mathsf{T}(\mathbf{x})$

48

is the normalized entity. This allows to include elements at infinity into the estimation process.

(b) Use the pseudo inverse of the spherically normalized entities as uncertainty matrix in the maximum likelihood estimation. As its null space $\boldsymbol{g}$ is known and normalized to 1, say $\boldsymbol{g} = \mathbf{x}^s$, it may be derived from, say

$$
\begin{bmatrix} \boldsymbol{\Sigma}^+_{x^s x^s} & \mathbf{x}^s \\[2mm] (\mathbf{x}^s)^\mathsf{T} & \mathbf{0} \end{bmatrix} = \begin{bmatrix} \boldsymbol{\Sigma}_{x^s x^s} & \mathbf{x}^s \\[2mm] (\mathbf{x}^s)^\mathsf{T} & \mathbf{0} \end{bmatrix}^{-1} . \tag{23}
$$

(c) In case iterations are necessary, change the covariance matrices of the spherically normalized observed entities to the fitted observations, say $\widehat{\mathbf{x}}$. I.e., use

$$
\boldsymbol{\Sigma}_{x^s x^s} = \boldsymbol{J}_s(\widehat{\mathbf{x}})\boldsymbol{\Sigma}_{xx}\boldsymbol{J}_s^\mathsf{T}(\widehat{\mathbf{x}})
$$

and its pseudo inverse from Eq. 23 with the null space of the fitted observations, say $\widehat{\mathbf{x}}$. This guarantees the external and internal constraints to be consistent (not shown in Fig. 8).
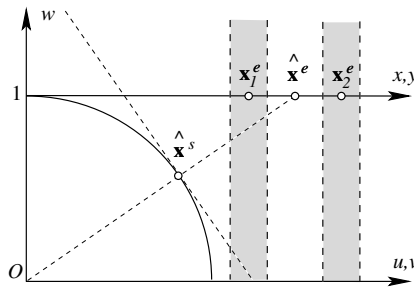
Fig. 7. Impossible situation for estimation: The shaded areas represent the confidence regions of the pseudo inverse of the classical covariance matrix of an Euclidean coordinate vector augmented by a fixed 1. Requiring the mean vector to be normalized to 1 yields severe inconsistencies (cf. text).
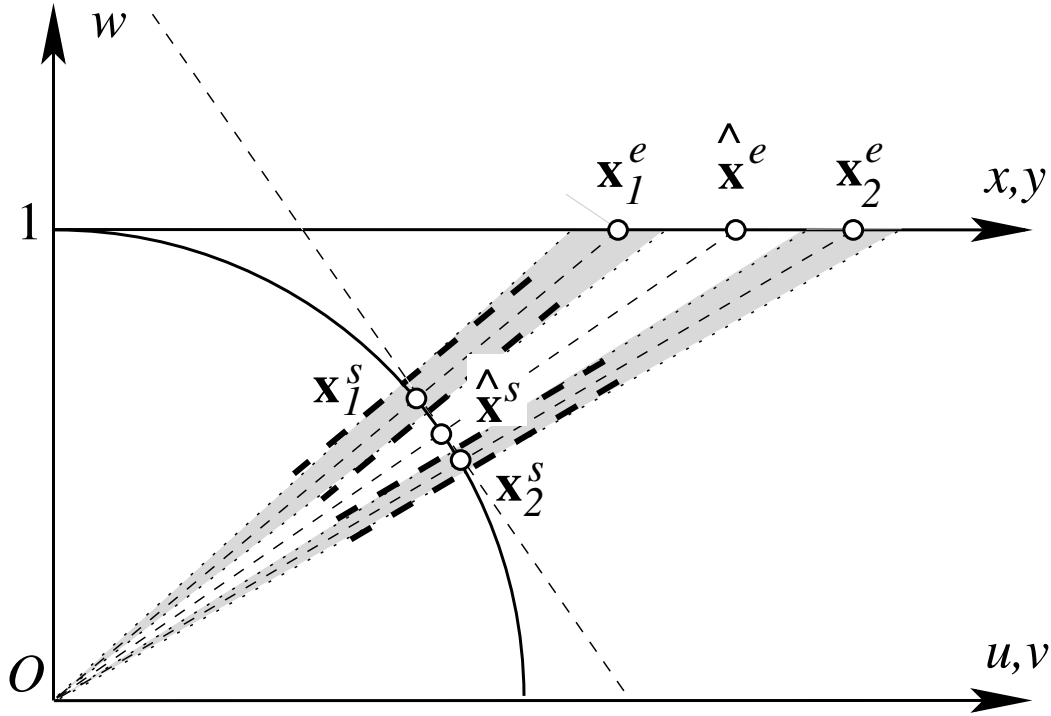
49

Fig. 8. Estimation with spherical constraint. The gray areas indicate the uncertainty of the observed points x_i. In the first iteration these regions are replaced by the two cylindrical regions indicated with the bold dashed lines, being parallel to the homogeneous vectors $\mathbf{x}_i$ or $\mathbf{x}_i^s$. In the following iterations, the two cylindrical regions will be oriented parallel to the estimated mean $\widehat{\mathbf{x}}^s$, being identical to the fitted observations $\widehat{\mathbf{x}}^s = \widehat{\mathbf{x}}_i^s, i = 1, 2$.

If the null space of the covariance matrix reflects the constraints on the observations the result with the pseudo inverse is the same as when minimizing the corresponding Euclidean version: If the rank of the covariance matrix of the n observations is r, one can always rotate the coordinate system of the $n = r + d$ observations, such that the r first observations have a full rank covariance matrix, and the other d have a zero-covariance matrix. Then the pseudo inverse just is the inverse of the first $r \times r$-block completed by zeros, indicating the last d observations have no influence on the result. In order to obtain defined values for the last d parameters one needs to include d constraints, which are a basis for the null-space of the covariance matrix.

50

As an example for Euclidean normalized points $\mathbf{x} = [x, y, 1]^\mathsf{T}$ the null space of the covariance matrix is $[0, 0, 1]^\mathsf{T}$ and thus the pseudo inverse, the weight matrix, does not weight the third component.

7.1.2 Estimation

Finding optimal estimates $\widehat{p}$ and $\widehat{l}$ for p and l respectively can be done by minimizing the Lagrangian

$$
\begin{aligned}
L(\widehat{v}, \widehat{p}, \lambda, \mu, \nu) = \frac{1}{2}\widehat{v}^\mathsf{T}\Sigma_{ll}^+\widehat{v} + \lambda^\mathsf{T}g(l + \widehat{v}, \widehat{p}) \\
+ \mu^\mathsf{T}h(\widehat{p}) + \nu^\mathsf{T}k(l + \widehat{v})
\end{aligned}
\tag{24}
$$

with the Lagrangian vectors λ, μ, and ν (Least-Squares-Adjustment).

For solving this non-linear problem in an iterative manner we need approximate values $\widehat{p}^{(0)}$ and $\widehat{l}^{(0)}$ for the unknown parameters $\widehat{p} = \widehat{p}^{(0)} + \widehat{\Delta p}$ and $\widehat{l} = \widehat{l}^{(0)} + \widehat{\Delta l}$. The corrections for the unknowns and the observations are obtained iteratively. With the Jacobians

$$
\begin{aligned}
A &= \left.\frac{\partial g(l, p)}{\partial p}\right|_{\widehat{p}^{(0)}, \widehat{l}^{(0)}} & K^\mathsf{T} &= \left.\frac{\partial k(l)}{\partial l}\right|_{\widehat{l}^{(0)}} \\
B^\mathsf{T} &= \left.\frac{\partial g(l, p)}{\partial l}\right|_{\widehat{p}^{(0)}, \widehat{l}^{(0)}} & H^\mathsf{T} &= \left.\frac{\partial h(p)}{\partial p}\right|_{\widehat{p}^{(0)}}
\end{aligned}
$$

and the relation $\widehat{l} = \widehat{l}^{(0)} + \widehat{\Delta l} = l + \widehat{v}$ we obtain the linear constraints by Taylor series expansion

$$
\begin{aligned}
g(\widehat{l}, \widehat{p}) &= g_0 + A\widehat{\Delta p} + B^\mathsf{T}\widehat{v} + B^\mathsf{T}(l - l_0) = 0 \\
h(\widehat{p}) &= h_0 + H^\mathsf{T}\widehat{\Delta p} = 0 \\
k(\widehat{l}) &= k_0 + K^\mathsf{T}\widehat{v} + K^\mathsf{T}(l - l_0) = 0
\end{aligned}
$$

with $g_0 = g(\widehat{l}^{(0)}, \widehat{p}^{(0)})$, $h_0 = h(\widehat{p}^{(0)})$, and $k_0 = k(\widehat{l}^{(0)})$.

Setting the partial derivatives (Eq. 24) zero yields the necessary conditions for a minimum

$$\frac{\partial L}{\partial \widehat{v}^{\mathsf{T}}} = \Sigma_{ll}^{+}\widehat{v} + B\lambda + K\nu = 0 \tag{25}$$

$$\frac{\partial L}{\partial \nu^{\mathsf{T}}} = K^{\mathsf{T}}\widehat{v} + K^{\mathsf{T}}(l - l_0) + k_0 = 0 \tag{26}$$

$$\frac{\partial L}{\partial \lambda^{\mathsf{T}}} = A\widehat{\Delta p} + B^{\mathsf{T}}\widehat{v} + B^{\mathsf{T}}(l - l_0) + g_0 = 0 \tag{27}$$

$$\frac{\partial L}{\partial \widehat{\Delta p}^{\mathsf{T}}} = A^{\mathsf{T}}\lambda + H\mu = 0 \tag{28}$$

$$\frac{\partial L}{\partial \mu^{\mathsf{T}}} = H^{\mathsf{T}}\widehat{\Delta p} + h_0 = 0. \tag{29}$$

These can be collected in the linear equation system

$$\begin{bmatrix} \Sigma_{ll}^{+} & K & B & O & O \\ K^{\mathsf{T}} & O & O & O & O \\ B^{\mathsf{T}} & O^{\mathsf{T}} & O & A & O \\ O^{\mathsf{T}} & O^{\mathsf{T}} & A^{\mathsf{T}} & O & H \\ O^{\mathsf{T}} & O^{\mathsf{T}} & O^{\mathsf{T}} & H^{\mathsf{T}} & O \end{bmatrix} \begin{bmatrix} \widehat{v} \\ \nu \\ \lambda \\ \widehat{\Delta p} \\ \mu \end{bmatrix} = \begin{bmatrix} 0 \\ -k \\ -g \\ 0 \\ -h_0 \end{bmatrix}.$$

with $k = K^{\mathsf{T}}(l - l_0) + k_0$ and $g = B^{\mathsf{T}}(l - l_0) + g_0$. The equation system can be reduced by applying

$$\begin{bmatrix} \Sigma_{ll}^{+} & K \\ K^{\mathsf{T}} & O \end{bmatrix}^{-1} = \begin{bmatrix} \Sigma_{ll} & K(K^{\mathsf{T}}K)^{-1} \\ (K^{\mathsf{T}}K)^{-1}K^{\mathsf{T}} & O \end{bmatrix} \tag{30}$$

to Eqn. 25 and 26 which yields the estimated corrections

$$\begin{aligned}\widehat{\boldsymbol{v}} = &-\boldsymbol{\Sigma}_{ll}\boldsymbol{B}\boldsymbol{\lambda}\\&-\boldsymbol{K}(\boldsymbol{K}^{\mathsf{T}}\boldsymbol{K})^{-1}\left(\boldsymbol{K}^{\mathsf{T}}(\boldsymbol{l}-\boldsymbol{l}_0)+\boldsymbol{k}_0\right)\end{aligned} \tag{31}$$

and the Lagrangian $\boldsymbol{\nu} = -(\boldsymbol{K}^{\mathsf{T}}\boldsymbol{K})^{-1}\boldsymbol{K}^{\mathsf{T}}\boldsymbol{B}\boldsymbol{\lambda}$. Eliminating $\widehat{\boldsymbol{v}}$ in Eq. 25 yields the Lagrangian

$$\boldsymbol{\lambda} = \boldsymbol{\Sigma}_{gg}^{-1}(\boldsymbol{A}\widehat{\boldsymbol{\Delta p}} - \boldsymbol{a}) \tag{32}$$

with the auxiliary variable

$$\begin{aligned}\boldsymbol{a} = &\boldsymbol{B}^{\mathsf{T}}\boldsymbol{K}(\boldsymbol{K}^{\mathsf{T}}\boldsymbol{K})^{-1}(\boldsymbol{K}^{\mathsf{T}}(\boldsymbol{l}-\boldsymbol{l}_0)+\boldsymbol{k}_0)\\&-\boldsymbol{B}^{\mathsf{T}}(\boldsymbol{l}-\boldsymbol{l}_0)-\boldsymbol{g}_0\end{aligned}$$

and the covariance matrix $\boldsymbol{\Sigma}_{gg} = \boldsymbol{B}^{\mathsf{T}}\boldsymbol{\Sigma}_{ll}\boldsymbol{B}$ of the contradictions.

By substituting $\boldsymbol{\lambda}$ in Eq. 28 we finally obtain the reduced normal equation system

$$\begin{bmatrix} \boldsymbol{A}^{\mathsf{T}}\boldsymbol{\Sigma}_{gg}^{-1}\boldsymbol{A} & \boldsymbol{H} \\ \\ \boldsymbol{H}^{\mathsf{T}} & \boldsymbol{O} \end{bmatrix} \begin{bmatrix} \widehat{\boldsymbol{\Delta p}} \\ \\ \boldsymbol{\mu} \end{bmatrix} = \begin{bmatrix} \boldsymbol{A}^{\mathsf{T}}\boldsymbol{\Sigma}_{gg}^{-1}\boldsymbol{a} \\ \\ -\boldsymbol{h}_0 \end{bmatrix}. \tag{33}$$

The estimates in the i-th iteration finally are $\widehat{\boldsymbol{p}}^{(i)} = \boldsymbol{p}^{(i-1)} + \widehat{\boldsymbol{\Delta p}}$.

7.1.3 *Precision of the estimation*

With estimated corrections $\widehat{\boldsymbol{v}}$ from Eq. 31 we obtain the fitted observations $\widehat{\boldsymbol{l}} = \boldsymbol{l} + \widehat{\boldsymbol{v}}$. The estimate for the variance factor σ_0^2 is given by the maximum likelihood estimate (Koch, 1999)

$$\widehat{\sigma}_0^2 = \frac{\widehat{\boldsymbol{v}}^{\mathsf{T}}\boldsymbol{\Sigma}_{ll}^{+}\widehat{\boldsymbol{v}}}{G + H - U} \tag{34}$$

with the number of constraints G, the number of restrictions H, and the number of parameters U. The pseudo inverse in Eq. 34 can eventually efficiently computed by exploiting the block diagonal matrix structure and the relation $\boldsymbol{K}^\mathsf{T}\boldsymbol{K} = \boldsymbol{I}$, i.e. $\boldsymbol{\Sigma}_{ll}^{+} = (\boldsymbol{\Sigma}_{ll} + \boldsymbol{K}\boldsymbol{K}^\mathsf{T})^{-1} - \boldsymbol{K}\boldsymbol{K}^\mathsf{T}$.

We finally obtain the estimated covariance matrix $\widehat{\boldsymbol{\Sigma}}_{\widehat{pp}} = \widehat{\sigma}_0^2 \boldsymbol{\Sigma}_{\widehat{pp}}$ of the estimated parameters, where $\boldsymbol{\Sigma}_{\widehat{pp}}$ results from the inverted reduced normal equation matrix

$$
\begin{bmatrix}
\boldsymbol{\Sigma}_{\widehat{pp}} & \cdot \\
\cdot & \cdot
\end{bmatrix}
=
\begin{bmatrix}
\boldsymbol{A}^\mathsf{T}\boldsymbol{\Sigma}_{gg}^{-1}\boldsymbol{A} & \boldsymbol{H} \\
\boldsymbol{H}^\mathsf{T} & \boldsymbol{O}
\end{bmatrix}^{-1}.
$$

7.1.4 *Iterative improvement*

For non-linear problems the approximate values have to be iteratively improved. For this the covariance matrix $\boldsymbol{\Sigma}_{ll}$ of the observations has to be adjusted for each iteration step by enforcing the constraints $\boldsymbol{k}(\boldsymbol{l}) = \boldsymbol{0}$ following Eq. 23 by spherical normalization.

A useful stopping criterion is that the maximal change of all $\widehat{\Delta p_j}^{(i)}$ in the i-th iteration should be less than a certain percentage, e.g. 1%, of the corresponding standard deviation, i.e., $\max_j \left(\left| \widehat{\Delta p_j}^{(i)} \right| \Big/ \widehat{\sigma}_{\widehat{p_j}}^{(i)} \right) < 0.01$.

7.2 *Relations to the Minimization of Algebraic Distances*

The estimation technique discussed above requires approximate values for the unknown parameters. Obtaining approximate values can be hard, especially if the functional relationships are non-linear. In case only one geometric entity is to be estimated, minimizing the algebraic distance can be a solution.

For the 2D geometrical entities discussed in this paper all constraints between the observations and the unknown parameters are linear in the parameters and homogeneous. Thus, we have the algebraic distances

$$\boldsymbol{A}(\boldsymbol{l}) \cdot \boldsymbol{p} = \boldsymbol{B}^{\mathsf{T}}(\boldsymbol{p}) \cdot \boldsymbol{l} = \boldsymbol{w}_g \overset{!}{=} \boldsymbol{0} \tag{35}$$

where the Jacobians depend only on the measurements or the parameters. Furthermore the restriction $|\widehat{\boldsymbol{p}}| = 1$, i.e., $(\widehat{\boldsymbol{p}}^{\mathsf{T}}\widehat{\boldsymbol{p}} - 1)/2 = 0$, is imposed on the homogeneous parameter vector which leads to $\boldsymbol{H}^{\mathsf{T}} = \widehat{\boldsymbol{p}}$.

However, considering the contradictions to be real i.i.d. observations we set $\overline{\boldsymbol{\Sigma}}_{gg} = \boldsymbol{I}$ and thus the corresponding eigenvalue problem becomes $\mu\widehat{\boldsymbol{p}} = \boldsymbol{A}^{\mathsf{T}}\boldsymbol{A} \cdot \widehat{\boldsymbol{p}}$. This solution minimizes the sum of the squared algebraic distances.

7.3 Optimal Estimation – An Example

After testing hypothesized mutual relations the grouping of points and straight lines is often the next step. This asks for an optimal joint estimation taking the uncertainties of the observations into account. Fig. 9 shows an example: The straight line l and the point χ, incident to l are to be estimated. The point is generated by intersecting straight lines m_i. The fitted straight line l results from observed incident points y_j, collinear straight lines n_k, orthogonal straight lines o_l, and parallel lines p_m.

7.3.1 Constraints and approximate values

We have the following constraints for the point

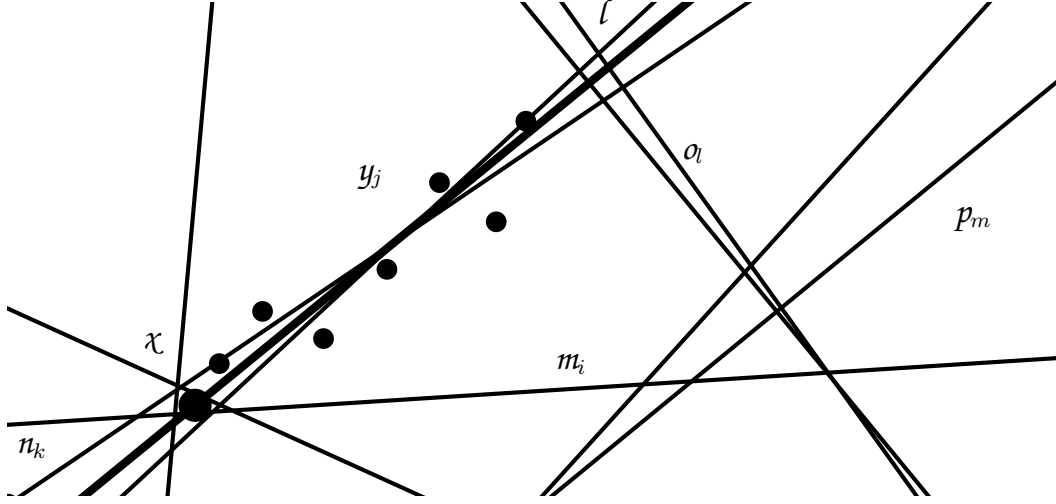$$\mathbf{x}^{\mathsf{T}}\mathbf{m}_i = \mathbf{m}_i^{\mathsf{T}}\mathbf{x} = 0 \qquad \forall \quad i$$

Fig. 9. Joint estimation of the point χ and the straight line l, being incident. The estimated entities are shown in bold. The point χ is determined by the intersecting straight lines m_i. The straight line l results from the observed incident points y_j, collinear straight lines n_k, orthogonal lines o_l, and parallel lines p_m.

and for the line

$$
\begin{aligned}
\mathbf{l}^\mathsf{T}\mathbf{y}_i = \mathbf{y}_i^\mathsf{T}\mathbf{l} &= 0 & \forall \quad j \\
\boldsymbol{S}_1^\mathsf{T}\mathbf{n}_k = \boldsymbol{S}(\mathrm{n}_k)\mathbf{l} &= \mathbf{0} & \forall \quad k \\
\mathbf{l}^\mathsf{T}C_\infty^* \boldsymbol{R}_\perp \cdot \mathbf{o}_l = \mathbf{o}_l^\mathsf{T} \boldsymbol{R}_\perp^\mathsf{T} C_\infty^* \cdot \mathbf{l} &= 0 & \forall \quad l \\
\mathbf{l}^\mathsf{T}C_\infty^* \cdot \mathbf{p}_m = \mathbf{p}_m^\mathsf{T} C_\infty^* \cdot \mathbf{l} &= 0 & \forall \quad m.
\end{aligned}
$$

The Jacobians with respect to the intersection point $\mathbf{x}$ and the straight line $\mathbf{l}$ are $\boldsymbol{A}_1^\mathsf{T} = \left[\ldots, \mathbf{m}_i, \ldots \right]$ and $\boldsymbol{A}_2^\mathsf{T} = [\ldots, \boldsymbol{S}_{\mathrm{n}_j}^\mathsf{T}, \ldots, C_\infty^* \boldsymbol{R}_\perp \mathbf{o}_k \ldots, C_\infty^* \mathbf{p}_l \ldots, \mathbf{y}_m, \ldots]$, thus $\boldsymbol{A}_1\mathbf{l} = \mathbf{0}$ and $\boldsymbol{A}_2\mathbf{x} = \mathbf{0}$, and the singular value decompositions (SVD) of $\boldsymbol{A}_1$ and $\boldsymbol{A}_2$ yield the approximate values.

7.3.2 Optimal estimation

The SVD solution neither takes the restriction $\mathbf{x}^\mathsf{T}\mathbf{l} = 0$ between the parameter vectors nor the uncertainties of the observations into account. The three restriction

equations are $\mathbf{l}^{\mathsf{T}}\mathbf{x} = 0$, $(\mathbf{x}^{\mathsf{T}}\mathbf{x} - 1)/2 = 0$, and $(\mathbf{l}^{\mathsf{T}}\mathbf{l} - 1)/2 = 0$. And with the parameter vector $\boldsymbol{p} = [\mathbf{x}^{\mathsf{T}}, \mathbf{l}^{\mathsf{T}}]^{\mathsf{T}}$

$$
\boldsymbol{H}^{\mathsf{T}} = \begin{bmatrix} \mathbf{l}^{\mathsf{T}} & \mathbf{x}^{\mathsf{T}} \\[2mm] \mathbf{x}^{\mathsf{T}} & \mathbf{0}^{\mathsf{T}} \\[2mm] \mathbf{0}^{\mathsf{T}} & \mathbf{l}^{\mathsf{T}} \end{bmatrix}, \quad \boldsymbol{h}_0 = \begin{bmatrix} \mathbf{x}^{\mathsf{T}}\mathbf{l} \\[2mm] (\mathbf{x}^{\mathsf{T}}\mathbf{x} - 1)/2 \\[2mm] (\mathbf{l}^{\mathsf{T}}\mathbf{l} - 1)/2 \end{bmatrix}
$$

holds for the general adjustment model. The Jacobian w.r.t. the observations

$$
\boldsymbol{l} = [\ldots, \mathbf{m}_i^{\mathsf{T}}, \ldots, \mathbf{y}_j^{\mathsf{T}}, \ldots, \mathbf{n}_k^{\mathsf{T}}, \ldots, \mathbf{o}_l^{\mathsf{T}}, \ldots, \mathbf{p}_m^{\mathsf{T}}, \ldots]^{\mathsf{T}}
$$

is the block-diagonal matrix

$$
\begin{aligned}
\boldsymbol{B} = \mathrm{Diag}\Big(&\ldots, \mathbf{x}^{\mathsf{T}}, \ldots, \mathbf{l}^{\mathsf{T}}, \ldots, \boldsymbol{S}_1^{\mathsf{T}}, \ldots, \\
&\ldots, \mathbf{l}^{\mathsf{T}}\boldsymbol{C}_\infty^*\boldsymbol{R}_\perp, \ldots, \mathbf{l}^{\mathsf{T}}\boldsymbol{C}_\infty^*, \ldots \Big)
\end{aligned}
$$

and the Jacobian w.r.t. the parameters is $\boldsymbol{A} = \mathrm{Diag}\,(\boldsymbol{A}_1, \boldsymbol{A}_2)$.

The fitted observations have to fulfill the condition $|\widehat{\mathbf{e}}| = 1$ for each observed geometric entity $e(\mathbf{e}) \in \{m_i, y_j, o_k, \ldots\}$. Since in this example each observed entity appears in one condition equation $\boldsymbol{g}(\boldsymbol{l}, \boldsymbol{p})$ at a time, the coefficient matrix $\boldsymbol{K}$ has block-diagonal shape, too. Therefore, $\boldsymbol{K} = \mathrm{Diag}\left(\mathbf{e}_1^{\mathsf{T}}, \mathbf{e}_2^{\mathsf{T}}, \mathbf{e}_3^{\mathsf{T}}, \ldots\right)$ and

$$
\boldsymbol{w}_k = \begin{bmatrix} \mathbf{e}_1^{\mathsf{T}}\mathbf{e}_1 - 1, & \mathbf{e}_2^{\mathsf{T}}\mathbf{e}_2 - 1, & \mathbf{e}_3^{\mathsf{T}}\mathbf{e}_3 - 1, & \ldots \end{bmatrix}^{\mathsf{T}}.
$$

Note, that for the conditions $\boldsymbol{S}_1^{\mathsf{T}}\mathbf{n}_k = \mathbf{0}$ linearly independent equations have to be selected each according to Eq. 22.

With the assumption of uncorrelated observed entities, the covariance matrix Σ_{ll} is a block-diagonal matrix. Together with the block-diagonal matrices A, B, and K the normal equation system 33 can be written as a sum of components which greatly reduces the computational costs (Heuel, 2004).

8   Conclusions and Outlook

For successful and efficient spatial reasoning a rigorous and consistent treatment of uncertainties is necessary because geometric entities derived from images are inherently uncertain. Feature extraction methods deliver entities and their uncertainties in various representations. Therefore, an overview of common representations for uncertain geometric entities and corresponding conversions has been given. Since uncertain straight line segments are a primary result of many feature extraction procedures, the set of point and straight line representations has been extended with representations for straight line segments.

Within the powerful framework of algebraic projective geometry the advantages of representing geometric entities with homogeneous coordinates together with their covariance matrices have become evident. Although the redundancy of the homogeneous representation leads to singular distributions, the benefits are manifold and remain valid also for uncertain entities:

- The homogeneous representation is generic and therefore yields a consistent set of representations for all types of uncertain entities.
- Homogeneous representations are suitable for all steps of geometric reasoning — no change of representation is necessary during image analysis. The other representations and their mutual conversions are discussed in order to (1) be able

to transform in the projective framework for uncertain spatial reasoning and (2) for exporting results together with their uncertainties.

- The resulting relations are simple and often bilinear in the observations and unknown parameters. This eases uncertainty propagation.

For the straight line segments no compact homogeneous representation is known to the authors. Yet, by representing them as aggregations of entities represented by homogeneous vectors, it is possible to treat them in the same way.

Within the different steps of geometrical reasoning homogeneous representations can be used efficiently:

- The construction of new entities from given ones is simple since the operations are mutual duals.
- Taking into account uncertainty is essential for hypothesis generation and verification. Statistical testing eliminates non-interpretable thresholds. The corresponding test statistics can easily be computed for homogeneous representations.
- For Maximum-Likelihood parameter estimation we provided a generic model which takes the observations, their individual uncertainties, and their correlations into account — this yields optimal results in the statistical sense. The adjustment model allows the estimation of multiple geometric entities, which is more general than the hitherto known procedures. It can incorporate hard constraints for the fitted parameters as well as for the fitted observations. Homogeneous representations for both, the parameters and the observations can be used with regular or singular covariance matrices. Extending the estimation process to a Bayesian one is straightforward.

The generalization of the representations and reasoning steps to 3D entities seems

to be straightforward though involving, especially concerning straight 3D lines and straight line segments.

Acknowledgment

References

Beder, C., 2004. Fast Statistically Geometric Reasoning About Uncertain Line Segments in 2D- and 3D-Space. In: Pattern Recognition. Vol. 3175 of Lecture Notes in Computer Science. Springer, pp. 375–382.

Bingham, C., 1974. An Antipodally Symmetric Distribution on the Sphere. Annals of Statistics 2 (6), 1201–1225.

Bronstein, I. N., Semendjajew, K. A., 1991. Taschenbuch der Mathematik. Teubner.

Chojnacki, W., Brooks, M. J., van den Hengel, A., 2001. Rationalising the Renormalisation Method of Kanatani. Journal of Mathematical Imaging and Vision 14 (1), 21–38.

Clarke, J. C., 1998. Modelling Uncertainty: A Primer. Tech. Rep. 2161/98, Department of Engineering Science, University of Oxford.

Collins, R., 1993. Model Acquisition Using Stochastic Projective Geometry. Ph.D. thesis, Department of Computer Science, University of Massachusetts, also published as UMass Computer Science Technical Report TR95-70.

Cormen, T. H., Leiserson, C. E., Rivest, R. L., 1990. Introduction to Algorithms. MIT Press.

Crevier, D., 1999. A Probabilistic Method for Extracting Chains of Collinear Segments. Computer Vision and Image Understanding 76 (1), 36–53.

Criminisi, A., 2001. Accurate Visual Metrology from Single and Multiple Uncalibrated Images. Distinguished Dissertations. Springer, London, Berlin, Heidelberg.

Duda, R. O., Hart, P. E., 1972. Use of the Hough Transformation to Detect Lines and Curves in Pictures. Communications of the ACM 15 (1), 11–15.

Estrada, F. J., Jepson, A. D., 2004. Perceptual Grouping for Contour Extraction. In: 17th International Conference on Pattern Recognition. Vol. 2. pp. 32–35.

Faugeras, O., 1993. Three-Dimensional Computer Vision: a Geometric Viewpoint. The MIT Press, Cambridge, Massachusets, USA.

Förstner, W., 2005. Uncertainty and Projective Geometry. In: Corrochano, E. B. (Ed.), Handbook of Geometric Computing. Springer, pp. 493–535.

Förstner, W., Brunn, A., Heuel, S., 2000. Statistically Testing Uncertain Geometric Relations. In: Mustererkennung 2000. Springer, pp. 17–26.

Förstner, W., Gülch, E., 1987. A Fast Operator for Detection and Precise Location of Distinct Points, Corners and Circular Features. In: Proceedings of the ISPRS Intercommission Conference on Fast Processing of Photogrammetric Data, Interlaken. pp. 281–305.

Fuchs, C., Förstner, W., 1995. Polymorphic Grouping for Image Segmentation. In: Proceedings of the International Conference on Computer Vision. pp. 175–182.

Guy, G., Medioni, G., 1996. Inferring global perceptual contours from local features. International Journal on Computer Vision 20 (1-2), 113–133.

Guy, G., Medioni, G., 1997. Inference of Surfaces, 3D Curves, and Junctions From Sparse, Noisy, 3D Data. IEEE Transactions on Pattern Recognition and Machine Intelligence 19 (11), 1265–1277.

Hartley, R., Zisserman, A., 2000. Multiple View Geometry in Computer Vision,

2nd Edition. Cambridge University Press, Cambridge.

Hartley, R. I., 1997. In defense of the eight-point algorithm. IEEE Transactions on Pattern Analysis and Machine Intelligence 19 (6), 580–593.

Helmert, F. R., 1872. Die Ausgleichungsrechnung nach der Methode der kleinsten Quadrate. Teubner, Leipzig.

Heuel, S., 2004. Uncertain Projective Geometry. Statistical Reasoning in Polyhedral Object Reconstruction. Vol. 3008 of Lecture Notes in Computer Science. Springer.

Jeffreys, H., 1961. Theory of Probability. Oxford University Press, London.

Kanatani, K., 1994. Statistical Analysis of Geometric Computation. CVGIP: Image Understanding 59 (3), 286–306.

Kanatani, K., 1995. Statistical Optimization for Geometric Computation: Theory and Practice, 2nd Edition. Artificial Intelligence Laboratory, Department of Computer Science, Gumma University, Japan.

Kanazawa, Y., Kanatani, K., 2001. Do We Really Have to Consider Covariance Matrices for Image Features? In: International Conference on Computer Vision. Vol. 02. pp. 301–306.

Koch, K.-R., 1999. Parameter Estimation and Hypothesis Testing in Linear Models, 2nd Edition. Springer, Berlin.

Köthe, U., 2003. Edge and Junction Detection with an Improved Structure Tensor. In: Pattern Recognition. Vol. 2781 of Lecture Notes in Computer Science. Springer, pp. 25–32.

Matei, B., Meer, P., 2000. A General Method for Errors–in–Variables Problems in Computer Vision. In: Computer Vision and Pattern Recognition. Vol. II. pp. 18–25.

McGlone, J. C., Mikhail, E. M., Bethel, J. (Eds.), 2004. Manual of Photogrammetry, 5th Edition. American Society of Photogrammetry and Remote Sensing.

Mikhail, E. M., 1976. Observations and Least Squares. University Press of America, Lanham, with Contributions by F. Ackermann.

Mühlich, M., 2005. Estimation in Projective Spaces and Applications in Computer Vision. Ph.D. thesis, Johann Wolfgang Goethe-Universität.

Neyman, J., Pearson, E. S., 1933. On the problem of the most efficient tests of statistical hypotheses. Philosophical Transactions of the Royal Society 231, 289–337.

Noronha, S., Nevatia, R., 2001. Detection and Modeling of Buildings from Multiple Aerial Images. IEEE Transactions on Pattern Recognition and Machine Intelligence 23 (5), 501–518.

Ochoa, B., Belongie, S., 2006. Covariance Propagation for Guided Matching. In: 3rd Workshop on Statistical Methods in Multi-Image and Video Processing (SMVP). On CD-ROM.

Rohr, K., 1992. Recognizing Corners by Fitting Parametric Models. International Journal of Computer Vision 9 (3), 213–230.

Schmid, C., Mohr, R., Bauckhage, C., 2000. Evaluation of Interest Point Detectors. International Journal of Computer Vision 37 (2), 151–172.

Shi, W., 1998. A Generic Statistical Approach for Modelling Error of Geometric Features in GIS. International Journal of Geographical Information Science 12 (2), 131–143.

Shi, W., Liu, W., 2000. A Stochastic Process-based Model for the Positional Error of Line Segments in GIS. International Journal of Geographical Information Science 14 (1), 51–66.

Utcke, S., 1998. Grouping based on Projective Geometry Constraints and Uncertainty. In: Sixth International Conference on Computer Vision. pp. 739–746.

Wolf, H., 1938. Über die Eigenschaft der plausibelsten Gerade einer fehlerzeigenden Punktreihe. Zeitschrift für Instrumentenkunde 11, 429–442.

Zhang, Z., 1998. Determining the epipolar geometry and its uncertainty: A review. International Journal on Computer Vision 27 (2), 161–195.